STARS

Electronic Theses and Dissertations, 2004-2019

2010

Experimental Analysis On The Effects Of Superficial Liquid And Gas Velocities In The Removal Of Hydrogen Sulfide From A Brine/oil Mixture

Joshua Lee

University of Central Florida

EXPERIMENTAL ANALYSIS ON THE EFFECTS OF SUPERFICIAL LIQUID AND GAS VELOCITIES IN THE REMOVAL OF HYDROGEN SULFIDE FROM A BRINE/OIL MIXTURE

by

JOSHUA D. LEE
B.S.M.E. University of Central Florida, 2008

A thesis submitted in partial fulfillment of the requirements
for the degree of Master in Science in Mechanical Engineering
in the department of Mechanical, Materials and Aerospace Engineering
in the College of Engineering and Computer Science
at the University of Central Florida
Orlando, Florida

Summer Term
2010

ABSTRACT

Hydrogen Sulfide (H_2S) is a harmful gas produced during petroleum extraction that leads to corrosion of drilling tools and pipelines. However, a H_2S-scavenging liquid compound, when added to pipelines, interacts with liquids that absorbed H_2S to create a non-corrosive bi-product. The interaction is associated with the mixing of gases and liquids. This thesis is a study on the effect of superficial gas and liquid velocities on the scavenger's efficiency. This study employs two experimental setups designed to simulate the mixing of gases and liquids within pipelines.

A high pressure closed loop was designed and fabricated to determine the influence of gas, liquid velocities and liquid volume on the scavenger's efficiency. All experiments were conducted in this high pressure loop with a thousand feet of coiled tubing to simulate the horizontal section of the pipeline that runs along the ocean floor from the reservoir. This provided practical understanding to petroleum companies to make a better forecast of how the scavenger used in eliminating the H_2S, is affected in the process of transporting the liquids and gases from the reservoir to the surface. For an adequate analysis, experiments on four liquid and four gas velocities ranging from 0.2m/s to 0.5m/s and 0.4m/s to 1.1m/s respectively were conducted. Results in this study indicated that increases in superficial gas velocity at low superficial liquid velocity decreases the scavenger efficiency while the opposite is seen at high superficial liquid velocity. In addition, the H_2S mass absorption was not a function of liquid volume as would be seen in static reservoirs but more of a function of superficial liquid and gas

iii

velocities. With the scavenger interacting with the liquid absorbed H_2S, it was expected that the efficiency would increase with the increase in volume but in this study this was not the case.

The second experiment is a flow visualization loop which was designed to understand the flow regimes at high pressures. This was done by constructing four 25ft section hoses together with four foot long breaks for visualization. This provided a more fundamental study of the fluid's behavior inside the pipelines allowing for the creation of appropriate flow regime maps in air-water flow. A hundred experiments for two different pressures were conducted at the 25ft location. At high pressures, the flow regime map appeared to shift the transition zones.

ACKNOWLEDGEMENTS

I would like to give my deepest appreciation to my advisor Dr. Ranganathan Kumar who gave me invaluable guidance and opportunities. I would also like to thank Ben Patrick, Luis Zea, Hongxia, Ehsan Yakhshi-Tafti, and Jim Strater for their individual help and knowledge. Petrobras thank you for funding this research and given me the opportunity to further this field of study. To my wonderful girlfriend Thuy, I thank you and appreciate everything that you have done over the years and putting up with those long nights. You mean everything to me. Finally, to my family, I thank you for the unwavering support.

TABLE OF CONTENTS

LIST OF FIGURES

ix

LIST OF TABLES

CHAPTER ONE: INTRODUCTION

One of our most highly sought after natural resource is petroleum. Today millions of barrels of petroleum are packaged and shipped all over the world. However, either around land or sea, this prized resource is usually always locked under layers of homogeneous sediments [1]. As a result, in order to efficiently obtain oil from the ground, the process of extraction has to constantly be updated. One aspect in need of further study is the process of how oil is extracted from underwater reservoirs and the natural gas that accompanies this extraction.

Currently, oil platforms that exist under ocean waters are gathered through a series of pipelines. A segment of pipeline runs towards the bottom of the ocean floor either straight down or at an angle. Once the pipeline hits the ocean floor, it runs horizontally along the ocean floor to the top of the oil reservoir. Within these oil reservoirs their lies salt water (brine), petroleum, and natural gas [2]. The most common gasses within the reservoirs are Carbon Dioxide (CO_2) and Hydrogen Sulfide (H_2S). While both CO_2 and H_2S can have detrimental effects on the equipment, the aggravated corrosion conditions caused by H_2S when mixed with oil, brine and other gasses are responsible for some of the highest equipment failure rates in the petroleum industry. This is due to H_2S's characteristics as the catalysis for absorption of hydrogen into steel. Thus, the slightest amount of H_2S in contact with equipment can cause Sulfide stress cracking [3]. When in contact with the equipment for long periods of time, H_2S can cause problems such as pitting corrosion, uniform corrosion, sulfide stress cracking, stepwise cracking, hydrogen blistering, and corrosion fatigue in the equipment metal [4].

Over the years, researchers have developed many methods of eliminating H_2S concentrations within pipelines. Some of the most popular methods include the continuous and batch injection of various scavengers (solid and liquid) in pipelines, the liquid redox process, and the usage of Claus/tailgas systems with each having its negative and positive implications as well as limitations [5]. However, within the last decade, the injection of liquid scavenger has dominated the industry due to its' lower capital cost and higher efficiency [5]. Currently, the most commonly used types of scavengers are the Triazine-based H_2S scavengers. The liquid Triazine in the scavengers is an organic compound that's either 1, 2, 3-Triazine, 1, 2, 4-Triazine or 1, 3, 5-Triazine [6]. The use of this type of scavenger entails a highly complex chemical reaction with the H_2S absorbed into the liquid. The scavenger when in contact with H_2S, strips a single hydrogen atom creating a safer bi-product. Each molecule of Triazine scavenger can interact with numerous H_2S molecules leading to a higher amount of H_2S removal per scavenger injected. For maximum efficiency the scavenger needs to be in contact with the H_2S thus the chemical reaction is highly dependent on the mixing of liquid and gases. More precise is the direct liquid scavenger efficiency is dependent on the gas velocity and is sensitive to the changing gas flow [5]. By pulling the liquids from the reservoir through the horizontal piping where the scavenger is injected with a multi-phase pump, the velocities of each phase can be changed. These changes can lead to different flow regimes which ultimately effect the mixing of both liquid and gases.

The scavenger amount (which is costly) put into the pipelines is a function of the H_2S concentration, the superficial velocities of both gas and liquid, and the volume of liquid. For each one of these reservoirs a different concentration of H_2S can be experienced which is

2

uncontrollable but the superficial velocities in which the liquids and gases are brought to the platform can be controlled. As a result, it is of grave importance to better understand the superficial liquid and gas velocities effects on the removal of H_2S.

The objective of this research was to investigate the effects superficial velocities have on the overall efficiency of the scavenger and the mass absorption of H_2S into the liquid. This was done via a series of loops. The first one created a semi ideal situation that simulated the oil recovery from the reservoir to the platform. The second one mimicked the first loop with visualization sections to understand the data resulting from the effects of the different velocities, both liquid and gases, by adequately displaying the flow characteristics and mixing behavior that are associated with these velocities.

3

CHAPTER TWO: LITERATURE REVIEW

<u>H_2S and Scavenger Effects</u>

Oil platforms all over the world gather oil from under the ocean through a series of pipelines. Within these oil reservoirs, exist various concentrations of hydrogen sulfide and carbon dioxide. Hydrogen Sulfide is not only harmful to pipe equipment due to its' corrosive characteristic but also harmful to humans and the environment [7]. Due to these side effects, regulation standards mandate that the maximum allowable H_2S concentration in gaseous be only four parts per million, (ppm) or less [8]. Since the concentration of CO_2 relative to H_2S in the reservoir is often very large (percent levels CO_2 compared to a few ppm of H_2S), the removal of CO_2 is less economical [7]. As a result, there has been more focus on improving the cost effectiveness of removing H_2S [7]. While researchers have developed many forms of eliminating H_2S concentration to allowable levels, liquid non-recoverable H_2S scavenger has been used most frequently in sour gas-oil reservoirs over the past decade [9].

Within the non-recoverable H_2S scavenger family, exists many types of scavenger such as Triazine, Acrolein, zinc oxide, and nitrites to name a few. In choosing the appropriate scavenger, a list of factors needs to be considered, as seen in Table 1. In addition to these factors, the various mechanisms of how the scavenger reacts also need to be considered. When considering the factors that affect a scavenger's efficiency, we see that most of the scavengers show the same effectiveness. However, Wilson's research indicates that Triazine scavengers may have a slightly more effectiveness over other scavengers [10].

4

Table 1: A List of factors contributing to scavenger selection [7], [8]

Factors Affecting Hydrogen Sulfide Scavenging
1. Production ratios between gas/water/condensate
2. Phase distribution
3. Operating temperature and Pressure
4. H2S Levels, actual and desired
5. Mixing efficiency
6. Contact time between the scavenger and gas
7. Chemical interference
8. Volume of petroleum present

As a result, many companies have leaned towards the Triazine based scavenger when compared to zinc oxide, nitrates and various amines scavengers as seen in Figure 1 [5], [10]. The process of producing Triazine based scavengers involves a reaction between formaldehyde and an alkanolamine comprising of 1 to 6 carbon atoms [11]. This process is low cost and yields a product with numerous incentives, as seen in Table 2. Thus, it's no surprise that Triazine scavengers currently dominate the market in terms of sales.
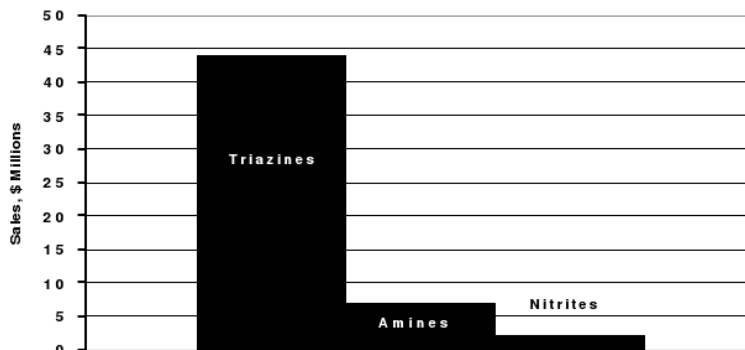
Figure 1: Liquid Scavenger Sales [5]

5

Table 2: Factors Contributing to Triazine scavenger usage [7].

Incentives for Triazine Scavengers
1. Selectivity towards H2S
2. Cost effective removal of H2S
3. Simplicity of operation
4. Adaptability to existing process equipment
5. Low toxicity and non-hazardous waste

The usage of scavenger entails a chemical reaction between the scavenger and H_2S absorbed inside liquids in the loop. This reaction forms organic polysulfides, trithianes, and a variety of other reaction products which are a safer bi-product [8], which is beyond the scope of this experimental research. By pulling the liquids from the reservoir through the horizontal piping where the scavenger is injected, as far upstream as possible [10] with a multi-phase pump, the velocities of each phase (liquid and/or Gas) can be changed. These changes can lead to different flow regimes which ultimately can cause insufficient mixing. This insufficient mixing can give the scavenger poor performance [9]. In addition, the direct liquid scavenger is dependent on the gas velocity and is sensitive to the changing gas flow [5]. As a result, the importance of understanding the effects of the liquid and gas superficial velocities on the system is critical. It is known that these velocity changes affect the flow regimes, but also controlling these changes in the flow regimes are other system parameters. Some of the other effects on the scavenger's efficiency include factors such as tubing diameter, injection velocity, and the kind of injection [12]. In this study a constant 1in diameter tube with a batch scavenger injection method will be utilized. This represents a semi-ideal case that might be seen in the industry.

6

Parameter Effects on Multiphase Flow Regimes

Although multiphase flow has been studied for many years, the physics behind such a flow is still not fully understood. Yet, many industrial processes rely on this phenomenon for material processing, petroleum processing, paper-pulping, power plants, and much more. In an ideal situation, if all pipes used in industry were perfectly horizontal, the flow would be naturally stratified with the less dense liquid (oil) occupying the upper part of the pipe and water the lower part [13]. However, since multiphase physics is very complicated in nature this is not the case. As a result, flow regime maps are needed and this experimental study is to investigate multiphase flow through horizontal pipes.

These flow regime maps help determine the physical flow patterns that are to be expected for a given combination of liquid and gas velocities. The importance of knowing these flow regimes for a given test, especially for this experimental study, is that each flow regime contains a unique flow characteristic that cause its own mixing behavior between the liquid and gas. This will show where the maximum efficiency for H_2S removal occurs not only in the individual flow regimes but on the entire flow regime map as a whole. Some of the more common flow regimes are shown on the left of Figure 2. The more common flow regimes are bubble, slug, stratified, wavy, and annular flows. Researchers have also incorporated two to three different types of flow regimes within one of the main flow regimes as seen on the right of Figure 2 [14]. Generally, different flow regimes induce different performances of the system. In addition, the highly non-linear nature of the forces which rule the flow regime transitions makes predictions difficult. As a result, there's a need for multiple flow regime maps tailored specifically for an application [15]. However, in addition to the different flow regimes needed specifically for various systems,

how these regimes are arranged on the velocity maps for various parameters is also significant. Fluid flow in the wellbore is influenced by several factors, including pipe diameter, flow rate, fluid types, fluid density, pipe orientation, liquid viscosity and pressures [13]. Some of the more popular studies that have been done in understanding these influencing factors for flow regime maps have been for pipe orientation, pipe characteristics and liquid characteristics. This study will look into the influence of one of the factors, the effects of pressure on the transitions of flow regimes.
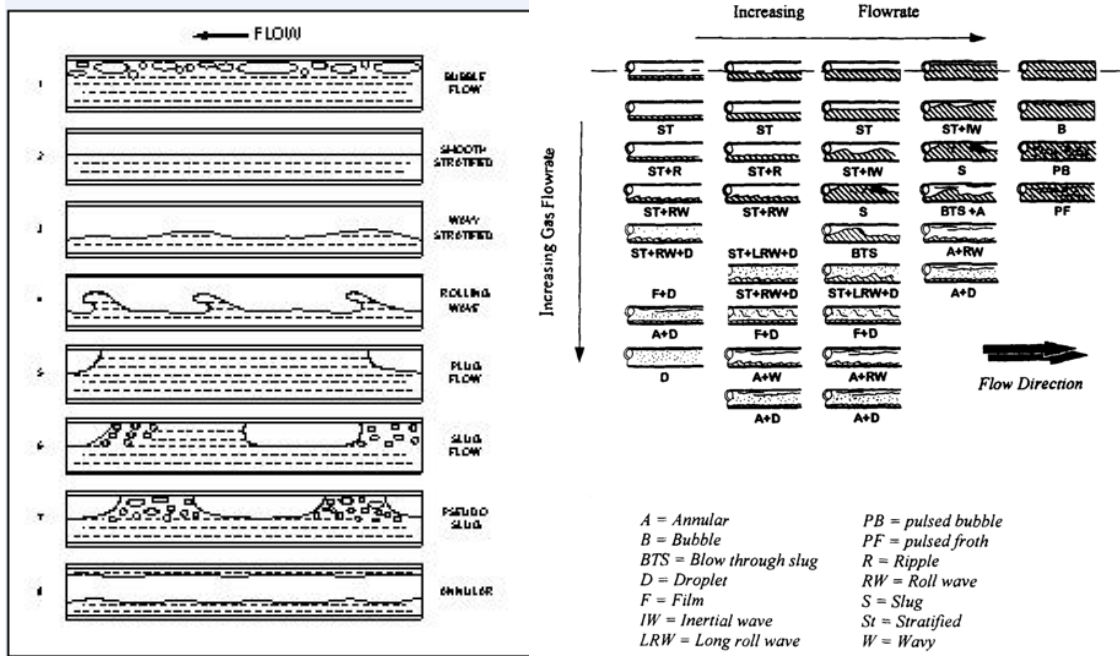
Figure 2: Left: Typical flow characteristics for multiphase flows, Right: More in depth flow regimes [13]

Pipe Orientation

In past studies, pipe orientation has always been horizontal or vertical. Some of the case studies for horizontal flow [16], [17], [18] used oil and water as the liquid interface. Each one of these studies have come across roughly the same flow patterns, stratified wavy, three layer, stratified mixed/oil, slug flow, and occasionally annular flows. For studies consisting of only water and air the flow patterns were as follows: dispersed bubble, slug, churn, and annular flows. For horizontal flows in general, it was noted that part of the main flow regimes within the map are consistent with each other. The discrepancy between the two comes from the oil viscosity and the wetting properties of the pipe walls [17], [18]. Thus, the wetting properties only had an effect when two extreme viscosities of oil were tested [18].

Another pipe orientation that has been studied is the vertical placement of the pipe. Most of the research has been done on solely water and air. Vertical multiphase (oil, water, gas) flows are often encountered in real work applications. In most cases the scavenger is injected into the horizontal section of the pipeline, thus the study of oil and vertical orientation of the pipe on the flow regime maps were not as important. Due to this underdeveloped area, a clear comparison on the effects of oil on vertical pipe flow regime maps cannot be made. For vertical pipe placement the most common flow patterns was bubbly flow, slug flow, churn flow, annular flow, and annular-mist flows [19], [20]. In Figure 3, the difference of the two orientations can be seen. Although the results done in the literature [19], [20] were different than that of Figure 3, due to the different parameters being considered, the overall idea of how the flow regime changes with respect to the pipe orientation is the same.
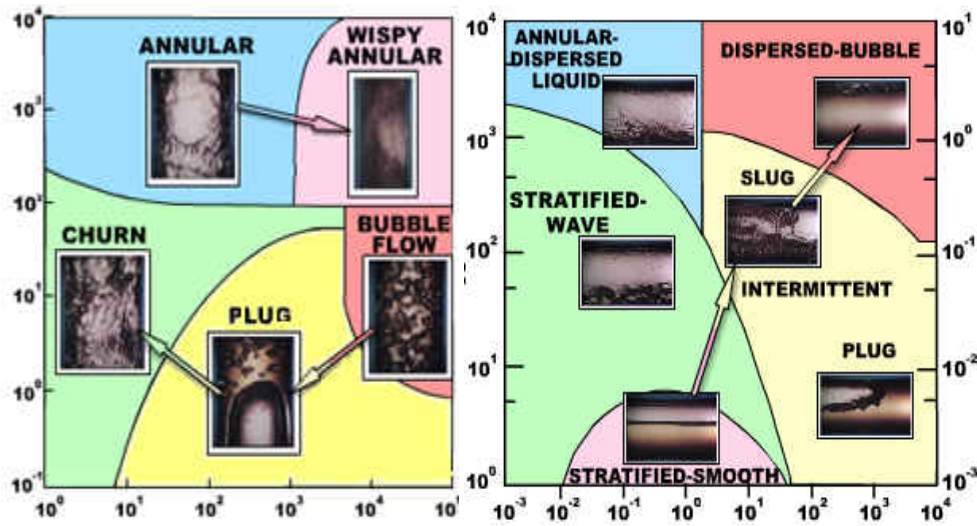
Figure 3: General overview of a flow regime map. Left: Vertical pipe orientation, Right: Horizontal pipe orientation

Despite these studies, having a completely horizontal or vertical pipe is extremely difficult in real world situations. Most oil pipe lines that run from the oil reservoirs to the platforms are rarely perfectly horizontal or vertical. Thus research [21], [22] has been conducted on the effects of inclined pipes. It has been noted that with even small deviations 1° or even less from the horizontal or vertical position a dramatic effect on the flow behavior, particularly at low flow rates can happen [12]. For the most part, with various inclination angles the following flow patterns were experienced: bubble, churn, elongated-bubble, slug, stratified, and stratified wavy flows [21]. Although these flow patterns are very similar to results from horizontal or vertical pipes, the difference comes with the inclination angle. For inclination angles of up to 5° only bubble and elongated bubble flow is experienced and at a 45° inclination only elongated bubble flow with some slug and churn flows were experienced [21]. With each pipe orientation a new

set of flow patterns are experienced, thus further research is needed to better understand other significant parameters.

Pipe Characteristics

Another highly researched area in the development of flow regime maps is the effect various pipe characteristics have on the flow patterns. This incorporates various pipe geometries such as round, square, rectangle, and triangle cross-sections [23], [24] and even a helical pipe configuration [25]. Some of the other pipe characteristics looked at was the size of the pipe such as capillary tubes [26], [27], small to medium pipes, [19], [20], and large pipes [21], [22]. It has been discovered that when comparing different pipe geometries that have the same hydraulic diameter, flow regime transitions are not so different from traditional round geometries [24]. Even in the extreme case of a triangular cross-section the flow patterns encountered was very similar to that of traditional round cross-sections [23]. Zhao and Bi [23] also found that when the hydraulic diameter decreases towards the capillary size some of the traditional flow regimes were not experienced. Thus, many researchers have concluded that flow regimes are not affected solely on the pipe geometries but more on the pipe size in itself. The effects can clearly be seen in Figure 4 illustrating the flow regimes generated by Misaim and Hibachi [19]. The effect of the diameter does not play an important role in the overall flow patterns but does towards shifting the transition lines of where the flow patterns reside on the map. This has been tested by others such as Hue, Chen, Tian, and, Karayiannis. [20]. Even if one approaches the capillary level, the same effect is seen with the difference coming from the flow pattern details being a little different than larger diameters due to the surface tension playing a greater role [27]. Overall the

11

importance of pipe characteristics on the flow patterns lies more in the diameter size than the actual cross-sectional geometry.
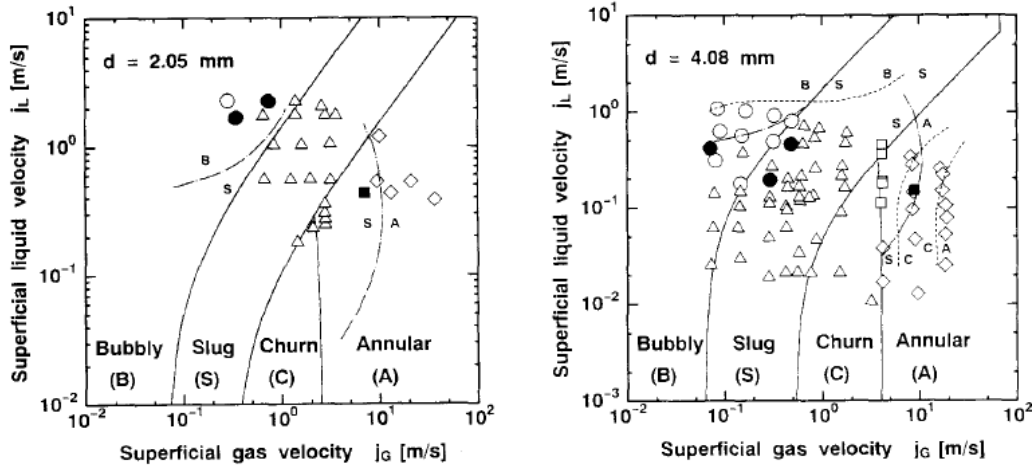
Figure 4: Vertical flow regime maps for different diameters [19], Left: D=2.05mm, Right: D=4.08mm [19]

Liquid Characteristics

Liquid characteristics such as type of liquid, density, and liquid viscosity are all important factors in the flow regime development. The liquid characteristic that will be looked at in depth are the effects the different types of liquids have on the flow patterns. A good comparison can be made from the maps generated by Coleman, Garimella, and Srinivas [24], Triplett, Ghiaasiaan, Abdel-Khalik, and Sadowski . [26], and Wenhong, Liejin, Tiejun, and Zhang. [17].

12
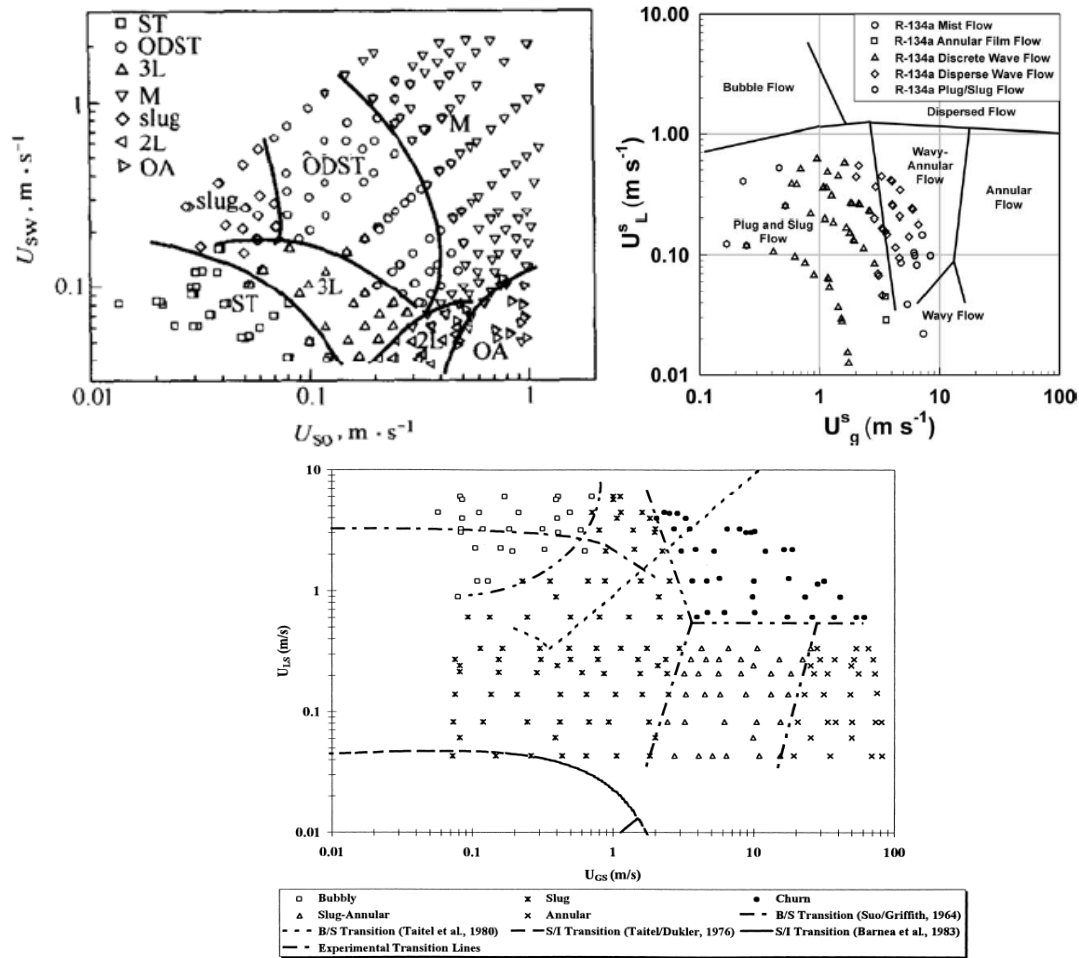
Figure 5: Flow Regime maps for various liquids; Top Left: Oil &Water [17], Top Right: R-134a [24], Bottom Center: Water [26]

These given maps were developed from similar parameters thus the only difference in the maps are the liquid type inside the loop. Although the oil flow regime map does not go to the same velocity scale as the other two, it is still seen that the flow regimes observed was dramatically different. The other two maps have similar transition lines with the R-134a having more flow regimes identified but overall the main flow patterns are the same. This can only suggest that the flow patterns are mainly affected by the viscosity of the liquid.

13

With the understanding of how different system parameters can affect the flow regime it is important to find the scenario the best fits the experimental study at hand. This experimental study will consist of high viscosity oil, water, and 1in helical/horizontal pipe at 20bars. All of these system parameters have been explored in past except for the system pressure. Thus the focus of this research is to take a simple flow regime map setup and analysis the effects of system pressure.

CHAPTER THREE: MATERIALS AND METHODOLOGY

Scavenger System: Hardware

The scavenger system is a simulation of the first thousand feet of horizontal piping that pulls the oil from the reservoir to the platform. The main component of the test apparatus is a progressive cavity multi-phase pump with 1000ft of continuous 1.0" OD 316 stainless steel rated to work at a maximum pressure over 1500psi. The entire loop consists of a total volume of ~45gallons.

Figure 6: Scavenger system in the beginning

This is adjoined by several gas tanks, monitors, and storage or mixing tanks as shown in Figure 7. All pipe fittings, valves, and hoses were either 1010 carbon steel or 316 stainless steel. The hoses were made of Teflon. Both thread tape and sealant were used in every single thread with the aim of having redundancy for safety reasons. Throughout the closed loop laid two pressure relief valves that were placed at the beginning and end of the loop to ensure the system

15

never reached the maximum working pressure. All components throughout the system have been chosen due to their ability to work at high pressures and their corrosion resistance to H_2S.

Figure 7: Completed scavenger system

The correct ratios of brine to oil are to be inputted into the scavenger system via a pump. The pump being used is an air-driven Haskel ¾ HP (0.56kW). Its' maximum rated output pressure was 1500psi (103 Bar) with a 0.8 in^3 displacement/cycle.

16
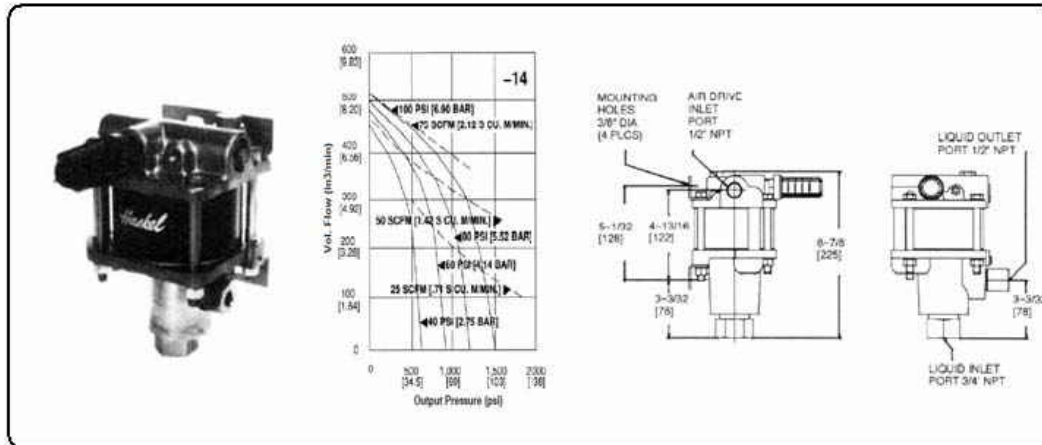
Figure 8: Haskel ¾ air-driven Pump

Along the 1000ft of continuous pipe two ports at different locations, 500ft and 1000ft are built for sample collecting at two different contact times (time the scavenger is interacting with the H_2S). Each one of these sections was used to collect a sample of the gas at high pressure in the loop. As seen in Figure 9, each sample collector is made of 1010 carbon steel. In addition, all tees, nipples, and other pipe fittings were scheduled 80 to allow for high pressures. At the top of the sample collector Teflon hoses were used to connect the sample collector to the regulator which brings the pressure down to atmosphere so that the H_2S sensor can get an adequate reading.

17

Figure 9: The 500ft sample collector

For scavenger injection, another high pressure vessel was attached to the beginning of the loop. All pipe fittings were constructed of scheduled 80 requirements. This high pressure chamber had a release valve at the top to bleed the vessel of the high pressure and bring it back down to atmosphere pressure for other testing that require different scavenger amounts.

Figure 10: Scavenger injection vessel

18

.
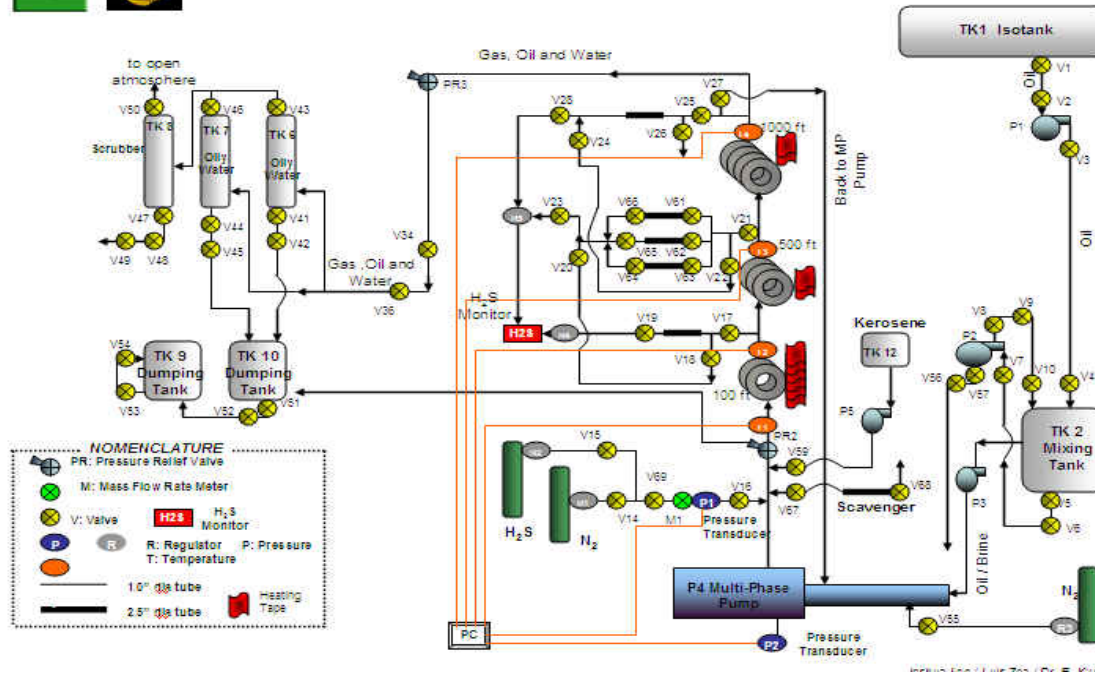
Figure 11: Scavenger system schematic

As seen in Figure 11, the scavenger system has one hydrogen sulfide sensor that connects to both sample collectors for consistency purposes. These sensors are Gas Alert Extreme electrochemical cell H_2S sensors with a 0-100ppm range with 1ppm display accuracy. As seen in Figure 12, these sensors only need a sample of ~90seconds to adequately display the concentration of gas in the sample collector. To bleed the gas into the sensor, a Harris HP 742 two stage stainless steel regulator is connected to the sample collector that will deliver the high pressure gas to the sensor at atmosphere pressure. This same regulator is used to deliver the H_2S gas into the loop to initially set up the experiment.

19
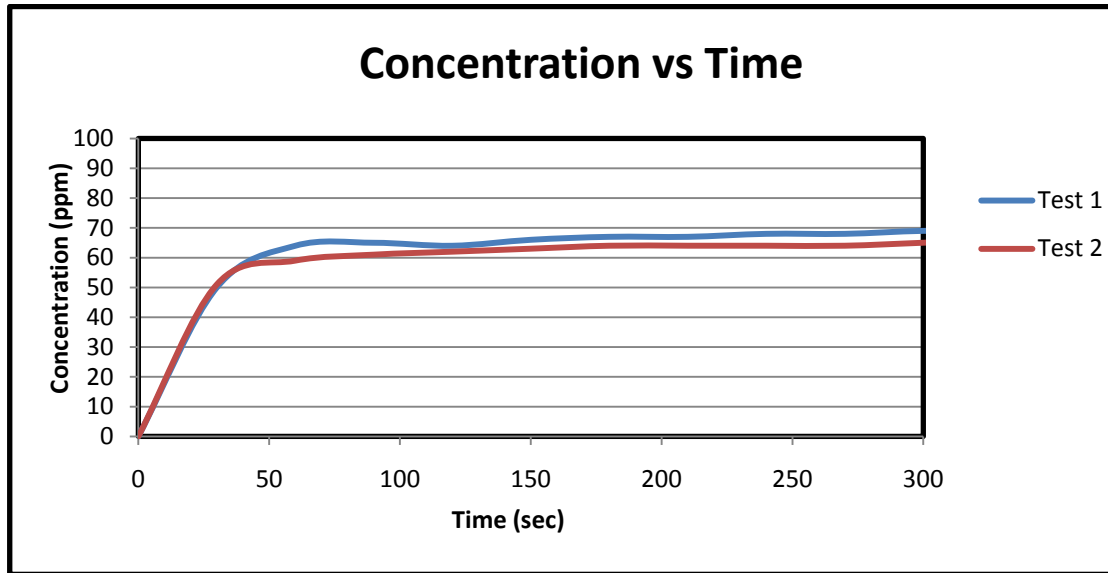
Figure 12: Sensor detection time

Once the experiment is completed the loop must be bled through a series of tanks that will scrub the H_2S out of the system so that the pressure can be released into the atmosphere. The tanks shown in Figure 13 are used to temporarily hold the liquids that were inside the loop during the experiment. Once all the gases and liquids have been let out of the system, the liquids in the temporary liquid holding tank are transferred to a bigger more permanent stainless steel waste tank.

20

Figure 13: Scrubbing system, Tanks 6, 7, 8.

Chemicals Used

Brine

Brine is a highly concentrated form of saline solution which is commonly known as sea water. This liquid is a common occurrence in many petroleum reservoirs. For direct simulation purposes all experiments contained brine instead of plain water. Each experiment consisted of the same composition as sea water which is a 2% volume solution. From the calculation below this came out to be 43grams of salt per liter of water. .

$$0.02x\left(\frac{1000\,ml}{1L}\right)\left(\frac{1cm^3}{1ml}\right)\left(\frac{1ml^3}{100^3cm^3}\right)\left(\frac{2170\,kg}{1m^3}\right)\left(\frac{1000\,g}{1Kg}\right) = 43g/L \qquad (1)$$

Nitrogen

Nitrogen is the most abundant natural gas in the atmosphere composing of nearly 78% of the atmosphere. This gas has the characteristics of being odorless, colorless, and tasteless. It is also

21

an inert gas. Due to its' inert behavior it was used to balance out the hydrogen sulfide delivered into the experiment to achieve the required starting concentration of hydrogen sulfide.

Petroleum

Petroleum is better known around the world as crude oil. This liquid is usually very dark in color, flammable, and very sluggish with a high viscosity. This liquid has mild effects on the body but is highly encouraged to wash off immediately when direct skin exposure is present. In the world there exist four major types of oils: oil sands bitumen, conventional oils, heavy oil, and extra heavy oils. Both the conventional and bitumen oil take up 30% of the total oil each while 15% is heavy oil and 25% is extra heavy oil. For this experiment the oil that was used was heavy oil given by Petrobras an oil company in Rio de Janeiro, Brazil which is what they have excavated off of their coast.

Hydrogen Sulfide

This natural gas is not only corrosive but highly dangerous when inhaled. A few short breaths of concentrations around 500ppm or higher can cause death. This gas has the characteristics of being colorless and is well known for its rotten egg scent when smelled at low concentrations. After a certain concentration level (~100ppm to 300ppm) the smell fades away because the nose does not have the receptors to detect the gas at those concentration levels. With long enough exposure to such levels or even lower the possibilities of developing nose, throat, and eye irritation can occur. The use of this gas is to directly simulate a given condition in the petroleum reservoir.

22

Scavenger

Many forms of scavenger exist in the petroleum industry. The most commonly used is a liquid Triazine-based H_2S scavengers. This is due to their non-hazardous waste (product of the reaction) characteristics, its compatibility with current process equipment and low cost of H_2S removal [7]. Petrobras donated two types of scavengers that were to be utilized in their experimental analysis and due to confidentiality issue they are known as type K and W. Type K is a water (brine) soluble scavenger while type W is oil soluble. For the experiments at hand, since the majority of the fluid is brine type K was implemented throughout.

Scavenger System: Testing Procedure

To begin each set of data which is broken down into four sets the system must be clean from any memory effects that might be left over from previous experiments. This was done by inserting a mixture of kerosene and water into the multiphase pump using the Haskel pump. The system was also pressurized to 50psi. Once the liquids were inserted, the multiphase pump was used to drive the liquids through the loop for 30 minutes. About half way through the time the liquids were allowed to flow through the sample collectors to eliminate any memory effects. Once the time frame had elapsed the liquids were then sent through the scrubbing tanks to rid the system of the liquids. This procedure is then repeated but with only water.

To begin experimentation, all appropriate valves were closed and then opened; see Appendix A for complete instructions. After the checklist of the valves from appendix A is completed, an air driven Haskel pump was used to deliver the oil and brine mixture to the multi-phase pump at

23

2.4gals/min. Since the multiphase pump is a progressive cavity pump the volumetric flow rate is fixed whether it is liquid or gas present when set to a certain rpm. Therefore, the amount of liquid inputted into the system has a direct relationship to the superficial liquid and gas velocities. The ratio of superficial liquid velocity to total superficial velocity is exactly the same as the ratio of liquid volume to total volume, e.g. the case of the superficial liquid velocity (V_{SL}) of 0.215m/s and superficial gas velocity (V_{SG}) of 0.43m/s the total liquid volume (both oil and brine) in the loop would be 15gallons.

$$\frac{V_{SL}}{V_{SL}+V_{SG}} = .3333 = \frac{liquid\ volume}{Total\ volume} \tag{2}$$

Once the proper amount of liquid was placed inside the coils, the variable frequency drive on the multi-phase pump was turned on to the correct rpm speed that was calibrated to associate with the total superficial velocity. Hydrogen sulfide (1000ppm) was then injected into the loop. Due to the liquid absorption of H_2S, an incremental procedure was done to obtain the required initial concentration with the required final pressure. For this, a certain amount of H_2S was placed into the loop to mix with the liquids by the multiphase pump for approximately 30 minutes until equilibrium has occurred. Next, a sample from one of the sample collectors was gathered and delivered to the sensor for an adequate reading. Upon the sensors reading, either more H_2S was placed in the system to increase the initial concentration or nitrogen was placed into the loop to lower the H_2S concentration. Since the absorption of H_2S into the liquid is a function of pressure, liquid, and gas velocity small increments of H_2S and nitrogen is needed to set the initial concentration to the correct value while being at the correct system pressure.

24

With the initial concentration set, the next step was to prepare the Triazine based scavenger (Type K). The correct scavenger amount is based on the superficial velocities, volume of liquid, and H$_2$S concentration. The equation below illustrates this.

$$\frac{Initial\ H_2S\ Concentration\ \ (ppm\ )\times Concentration\ \ Ratio\ (35)\times Total\ Liquid\ Volume\ (L)}{1000000\ \times 1000} \tag{3}$$

The experimental concentration that was utilized throughout the testing was a 35:1 ratio. With the appropriate amount of scavenger being placed in the high pressure vessel along with a small amount of water (to ensure smooth injection into the loop), the valve leading to the pressurized loop was opened to release the scavenger into the liquid. The timer was then started. With knowledge of the speed of the liquid, the time for which the scavenger was to reach a desired location was achievable. A high pressure sample collector was built at the 500ft and 1000ft mark of the continuous coil. At the correct time when the scavenger reaches the sample collector, a liquid/gas sample from the coils is to be captured into the sample collector. Once the sample has been collected a stainless steel hose leading from the top of the sample collector to a regulator, delivering a constant flow of gas at roughly atmospheric pressure. A Gas-Alert monitor is then used to read the concentration of H$_2$S in the gaseous phase. The gas was left flowing for roughly 90 seconds for an accurate reading. After the reading was taken, the liquids and gases were allowed to flow through a few tanks for removal of liquids from the loop and scrubbing of the hydrogen sulfide in a 30% NaOH (Sodium Hydroxide) solution, which then goes to atmosphere. See appendix A for complete procedure.

The purpose of this analysis was to see what the scavenger's efficiency is with different combinations of superficial liquid and gas velocities. This was done by taking a simple

calculation into consideration. To obtain the scavenger efficiency, the difference of the initial concentration ($C_{H2S,i}$) and the final concentration ($C_{H2S,f}$) was divided by the initial concentration and multiplied by 100 to calculate the percentage.

$$\frac{C_{H2S,i}-C_{H2S,f}}{C_{H2S,i}} \times 100 = Scavenger\ Efficiency(\%) \tag{4}$$

To fully understand the scavenger's efficiency behavior with the change of the liquid and gas velocities a more in depth analysis is made pertaining to the absorption phenomena. It is important to first understand how much H_2S is being absorbed at different velocities before one can appreciate the scavenger's efficiency. In order to achieve this understanding a series of basic equations are utilized with the assumption of an ideal gas being considered.

In order to find the mass of H_2S that is absorbed into the liquid, equation (5) is utilized where V_{gas} (m^3) is the total gas volume and v_{H_2S} (m^3/Kg) is the specific volume of H_2S being placed into the loop.

$$m_{H_2S} = \frac{V_{gas}}{v_{H2S}} \tag{5}$$

Using equation (6) the total volume of gas in the loop can be determined.

$$V_{gas} = \frac{V_{SG}}{V_{SL}+V_{SG}} \times 45gal \times (\frac{0.003785\,m^3}{1gal}) \tag{6}$$

To find the specific volume of H_2S that is being placed in the loop a series of equations must be utilized. It is important to know that each H_2S tank being used has a concentration ppm value

26

attached to it and this value is that of a molar ppm value. For example if the tank is certified for 1000ppm then within the gas there lies 1000 moles of H$_2$S per million moles of Nitrogen. Knowing that the mole fraction is expressed as

$$x_i = \frac{n_i}{n_{tot}} = \frac{P_i}{P_{tot}} \tag{7}$$

Thus making the following equation for Hydrogen Sulfide:

$$P_{H_2S} = x_{H_2S}P_{tot} \tag{8}$$

where P$_{tot}$ is the total amount of pressure inserted from the H$_2$S tank. Now using the ideal gas equation of state, equation (9), the specific volume can be determined.

$$Pv = RT \tag{9}$$

Where the gas constant R is determined by the equation below:

$$R = \frac{R_u}{\overline{m}} \tag{10}$$

To solve equation (10) the universal gas constant $R_u = 8.314\ KJ/kmol * K$ and the molecular mass of H$_2$S ($\overline{m}$) must be used. To find the molecular mass of H$_2$S equation (11) must be used.

$$H_2S \rightarrow 2H + S \rightarrow 2(1.008\ g/mol) + (32.065\ g/mol) = 34.08\ g/mol = \overline{m}_{H_2S} \tag{11}$$

27
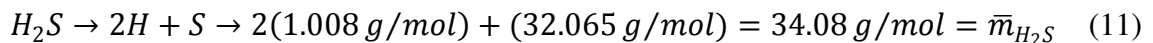
thus

$$R = \frac{8.314 KJ/kmol * K}{34.08 Kg/Kmol} = 0.244\ KJ/Kg * K \tag{12}$$

With all tests being conducted at room temperature (298K) the ideal gas equation (9) with equation (8) incorporated in it, is used to solve for the specific volume of H₂S.

$$v_{H_2S} = \frac{RT}{P_{H_2S}} = \frac{RT}{P_{tot}\,x_{H_2S}} = \frac{(0.244\,KJ/Kg*K)(298K)}{P_{tot}\,x_{H_2S}} = \frac{72.71\,KJ/Kg}{P_{tot}\,x_{H_2S}} \tag{13}$$

For sanity purposes a unit check is needed and is found that pressure needs to be in KPa while x_{H_2S} needs to have the units $mol/_{mol}$ to make dimensional sense.

With all needed values calculated the mass of H₂S can be found from equation (14)

$$m_{H_2S} = \frac{\frac{V_{SG}}{V_{SL}+V_{SG}} \times 45\,gal \times \left(\frac{0.003785\,m^3}{1\,gal}\right)}{\frac{72.71\,KJ/Kg}{P_{tot}\,x_{H_2S}}} \tag{14}$$

For each test run the initial concentration of H₂S ($x_{H_2S,i}$) was constant at 1000ppm while the partial pressure of H₂S (P$_{tot}$) and the volume of liquids and gas changed, thus the total mass inputted into the loop changes accordingly.

$$m_{H_2S,i} = \frac{V_{SG}}{V_{SL}+V_{SG}} \times 0.0234(m^3\,Kg/_{KJ})P_{tot}\,x_{H_2S,i} \tag{15}$$

28

Since the objective to each test was to get the starting concentration of H₂S ($x_{H_2S,f}$) to be 40ppm before the scavenger was placed into the loop the final concentration ($x_{H_2S,f}$) is known. With this being known the final mass of H₂S can be determined.

$$m_{H_2S,f} = \frac{V_{SG}}{V_{SL} + V_{SG}} \times 0.0234 (m^3 \, {}^{Kg}/_{KJ}) P_{tot} \, x_{H_2S,f} \tag{16}$$

With the initial and final mass of H₂S calculated the mass absorption by the liquids can be determined from equation (17).

$$m_{H_2S,absorbed} = \Delta m_{H_2S} = m_{H_2S,i} - m_{H_2S,f} \tag{17}$$

Due to the high toxicity of H₂S, the experiments were conducted with a vast amount of ventilation and proper gas mask. During the testing it was imperative to have all the doors that housed the system open to the atmosphere with industrial size fans constantly blowing.

Flow Visualization: Hardware

The flow visualization system is a simulation of the first hundred feet of the continuous thousand feet of stainless steel piping that makes up the scavenger system. The main components of the test system is a progressive cavity multi-phase pump, which is the same as the scavenger system multiphase pump and four sections of 25ft continuous 1.0" OD high pressure and oil resistant Teflon hoses that are rated to work at a maximum pressure of over 1000psi. The entire loop consisted of a total volume of ~8.5gallons. The completed setup can be seen in Figure 14.

Figure 14: Completed visualization loop.

All pipe fittings, valves, and hoses were 1010 Carbon steel and hoses made of Teflon. Both thread tape and sealant were used in every thread with the aim of having redundancy for safety reasons. Throughout the closed loop there are four transparent scheduled 80 PVC pipes for visual observation. To eliminate the distortion the camera would have when focused on a round tube, a clear box was built around the PVC pipes with the front piece having roughly the same refractive index as the PVC piping. A liquid substance (water) would then be placed inside this box to limit the drastic changes in the refractive index, as seen in Figure 15. All components throughout the system have also been chosen due to their capability to work at high pressures.

30

Figure 15: Flow observation box

To achieve the correct ratios of brine to oil, the same Haskel pump from the scavenger system was utilized. The Pump was once again an air-driven Haskel ¾ HP (0.56kW). Its maximum rated output pressure is 1500psi (103 Bar) with a 0.8 in^3 displacement/cycle.

The last major hardware of the system is a Fast-Tec Trouble Shooter high speed camera with a 2,000fbs capability which is placed directly in front of the clear PVC tubes as shown in Figure 16.
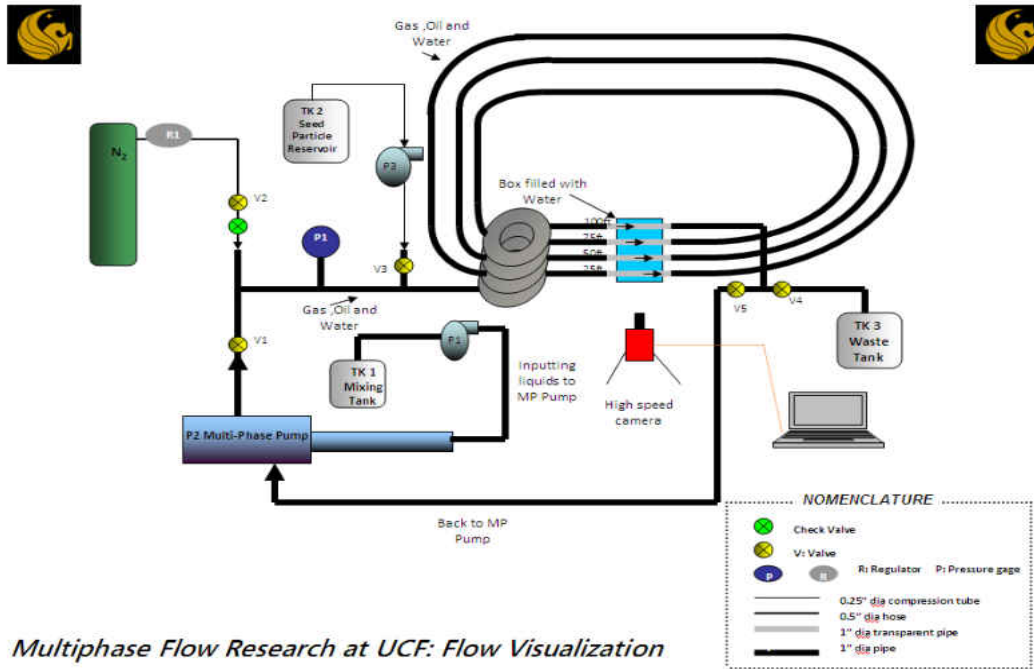
Figure 16: Flow visualization schematic

Once the experiments are completed the loop was then bled through a series of bypass hoses that removed the liquids from the system so that the pressure was released into the atmosphere (see appendix B). These hoses led to a 500gallon stainless steel waste tank. This tank is the same used for the scavenger system's waste.

<center><u>Chemicals Used</u></center>

Nitrogen

This natural gas is the most abundant gas in the atmosphere composing of nearly 78% of the atmosphere. This gas has the characteristics of being odorless, colorless, and tasteless. It is also an inert gas. Due to its' inert behavior and cost effectiveness, it is used to increase the pressure inside the visualization loop.

Petroleum

Petroleum is better known around the world as crude oil. The viscosity of the crude oil that was donated by Petrobras was ~497cp. Since this oil is completely black, it was not a favorable material to use inside the visualization loop. With this in mind, alternative oil was found. Standard SAE 40 motor oil was utilized for all visualization purposes due to its similar viscosity value of 525cp when compared to the donated crude oil. This motor oil is a light yellow in color and will allow for a better visualization through the tubes. Unfortunately when a series of test were run with this oil inside the visualization loop, emulsification happened due the high pressure thus was not utilized in this experimental study.

<center><u>Flow Visualization: Testing Procedure</u></center>

Before experimentation occurred, a new calibration curve was needed for the visualization loop setup with the multi-phase pump. The purpose of calibrating the pump was to correlate the rpm speed of the pump to the volumetric flow rate that the pump discharges. The calibration

<center>33</center>

process consisted of taking a bucket with a known amount of water and inserting it into the multi-phase pump. Then the pump is turned on to a certain rpm on the variable speed drive discharging a certain volume in a little time frame allowing for a volumetric flow rate to be calculated. This process is repeated several times until an adequate correlation was made between the rpm setting and the volumetric flow rate that is being pumped. This correlation is then modified to show the rpm setting to total superficial velocity. This process was an important calibration process because it gives an accurate way of telling which velocity correlates to which flow regime. Thus a volumetric flow meter was inserted into the loop. This would allow a more accurate calibration process and allow for the pressure adjustment to be considered. Once this is done the next procedure was carried out.

The experimental procedure for the flow visualization experiment was as followed. To start the experiment, the appropriate amount of water and oil was pumped into the multiphase pump by a Haskel pump. The Haskel pump is an air driven pump that delivers a flow rate of 2.4gpm when 40psi air is supplied. The total volume of the loop is roughly 8.5 gallons, so the ratio of liquid to gas needs to be inserted so that it gives the appropriate range of superficial velocities for both liquid and gases that needed to be looked at. The ratio of liquid to gas that is placed inside the loop is directly proportional to the ratio of liquid superficial velocity to superficial gas velocity (see equation 2). The total superficial velocity can be changed by increasing the rpm value on the variable speed drive of the multi-phase pump. However, the ratio cannot be changed unless a new ratio of liquid to gas is inserted into the loop. Once all the liquid is pumped into the loop, the pressure is then increased to the desired amount by injecting nitrogen into the loop. Once that was achieved, the multiphase pump was set to a certain rpm that correlates to a liquid

34

and gas superficial velocity that needed to be tested. After the pump was set, the liquid and gas are allowed to mix for a desired time to reach equilibrium (~15-20 minutes). Once the liquid and gas have reached equilibrium, the high speed camera was turned on and setup to zoom and focus on the tube with either a 500fps or 1000fps frame rate. After making sure that the camera was correctly working while looking at the correct section of the pipe, the record option was turned on and the images are captured for a few seconds. This was repeated for all the superficial liquid and gas velocity combinations for the given liquid to total volume ratio that are desired for the experimental study to be completed.

Once all the images for the test runs have been taken, they are processed using the high speed camera software to see the flow regimes at the given combination of superficial liquid and gas velocities. When all the different combinations of superficial liquid and gas velocities are done, a new ratio of liquid was inserted into the loop to give another range of both liquid and gas superficial velocities. This process was repeated for all combinations of superficial liquid and gas velocities that are being studied. This same procedure was then repeated for different starting pressures and different locations. Once that was done a simple flow regime map was generated from the images for various pressures.

CHAPTER FOUR: RESULTS AND DISCUSSION

Preliminary Results

Table 3 and 4 below consists of all the constant parameters and varying parameters for the experimental study. Since all reservoir conditions could not be tested, it was important to eliminate and find a series of constant parameters that will have the biggest impact with the velocities being studied. They were chosen via a series of preliminary tests.

Table 3: Constant Parameters

Constant Parameters	
Pressure	20 ± 0.66 bars
Water Cut (%)	80 ± 5
Initial H2S Concentration	40 ± 4ppm
Scavenger Volume Ratio	35:1

Table 4: Varying Parameters

Varying Parameters	
Superficial Liquid Velocity (m/s)	Superficial Gas Velocity (m/s)
0.215 ± 0.01	0.430 ± 0.01
0.322 ± 0.01	0.750 ± 0.01
0.430 ± 0.01	0.916 ± 0.01
0.537 ± 0.01	1.075 ± 0.01

Figure 17 shows how the two different scavenger concentrations affect the efficiency at 0.215m/s liquid and 0.43m/s gas velocities for a starting H_2S concentration of 40ppm. As one would expect, the graph shows that as the concentration amount increases the efficiency becomes higher. Within this test it was also noticed that the contact time is more critical for the lower concentration amount indicating that it takes a longer time for this amount of scavenger to reach

its' maximum potential. As a result, the higher scavenger concentration was chosen to be utilized for all tests being conducted.
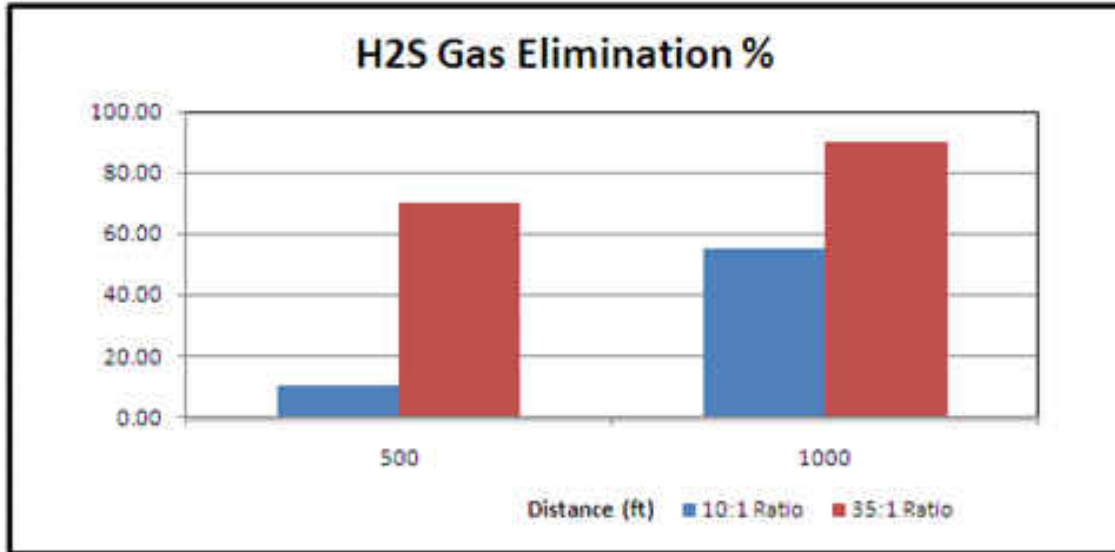
Figure 17: Preliminary Test: Vsl =0.215m/s, Vsg = 0.430m/s, 20bar, 80%WC, 40ppm

Figure 18 shows how the two different starting H_2S concentrations affect the efficiency at 0.215m/s liquid and 0.75m/s gas velocities for a starting pressure of 20bars while Figure 19 is for 70bars. It is observed that for lower starting pressure, the lower starting concentration resulted in a slightly better efficiency at lower contact time but became more distinct at a later contact time. Also, at lower concentration value, the increase in contact time caused a greater increase in the efficiency. Alternately, higher starting pressure showed similar results but a huge difference is seen between the two initial concentration values at both contact times. Accordingly, the increases in the efficiency at the two contact times were very similar to each other. From the results, it was concluded that the initial H_2S concentration had a significant impact on the

efficiencies at the different pressures. Since the lower initial concentration was greater for both pressures, 40ppm was used for the starting concentration for all tests.

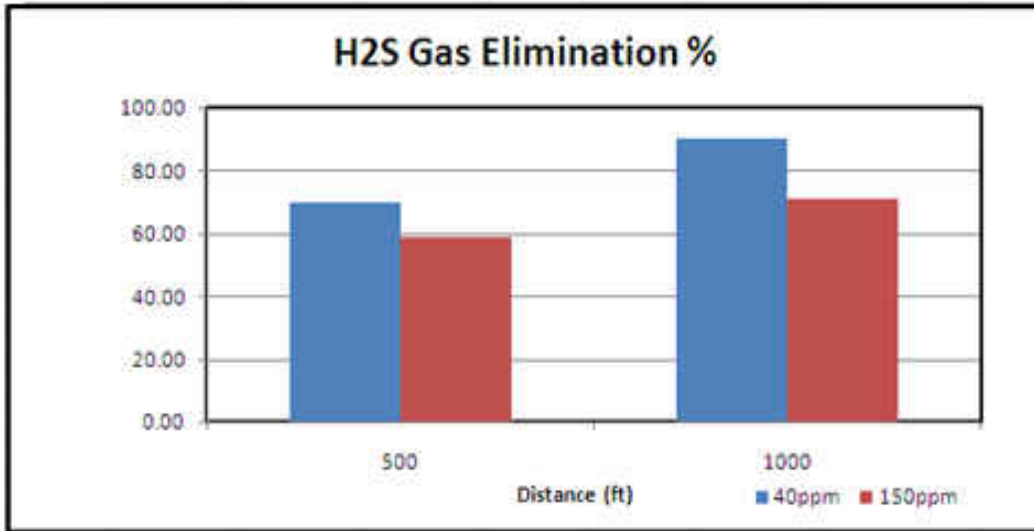**Figure 18: Preliminary Test: Vsl =0.215m/s, Vsg = 0.430m/s, 35:1 ratio, 80%WC, 20bar**
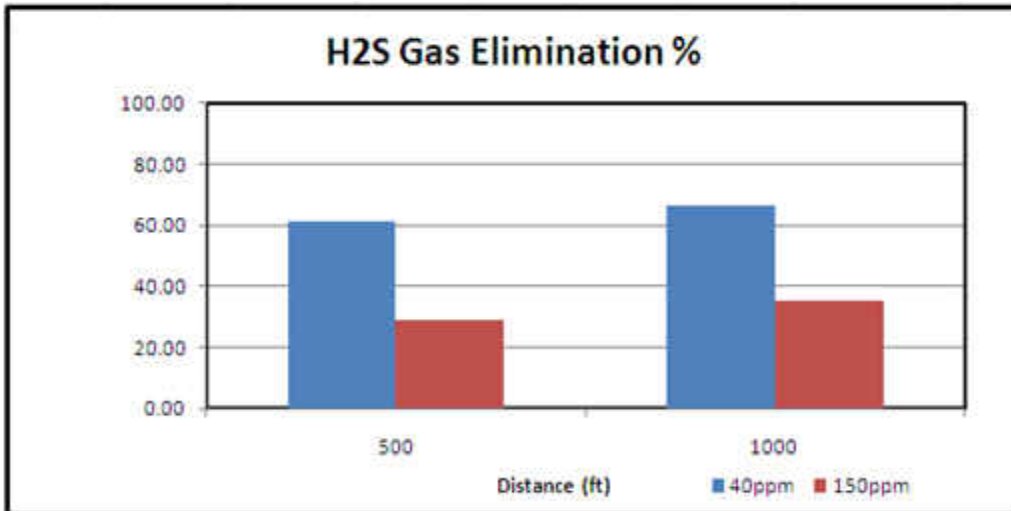
Figure 19: Preliminary Test: Vsl =0.215m/s, Vsg = 0.75m/s, 35:1 ratio, 80%WC, 70bar

38

Figure 20 shows how the two different starting pressures affect the efficiency at 0.215m/s liquid and 0.75m/s gas velocities for a starting H_2S concentration of 40ppm while Figure 21 is for 150ppm. It is observed that for the lower starting concentration value the higher pressure resulted in a slightly better efficiency at lower contact time but produced similar results at later contact time. Also, at lower pressure the increase in contact time caused a greater increase in the efficiency. Alternately, the higher starting concentration showed the lower pressure having a better efficiency but slower increase in efficiency with longer contact time. As a result, it was concluded that pressure had a greater impact on the higher concentration value while the lower concentration value which will be utilized throughout all tests showed little difference. Thus the lower pressure was chosen as a constant parameter for safety precautions.

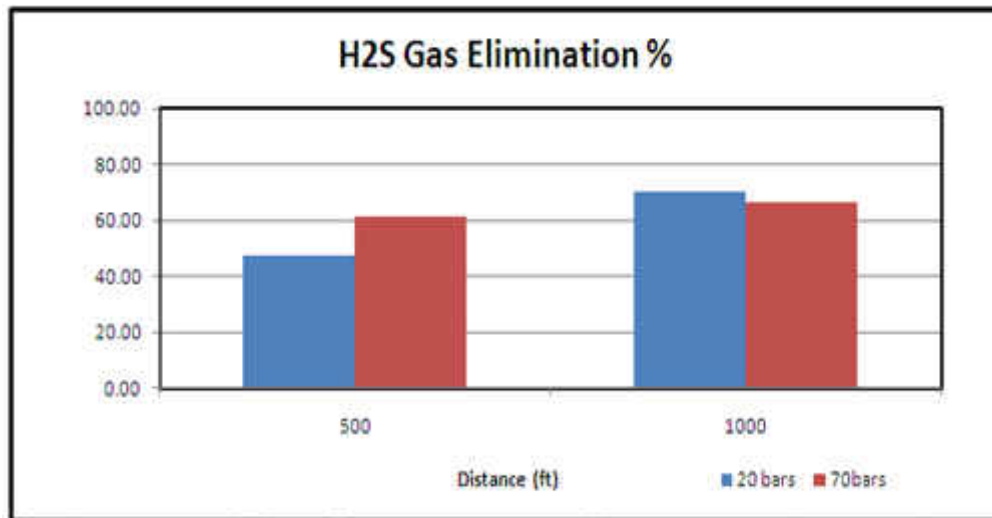**Figure 20: Preliminary Test: Vsl =0.215m/s, Vsg = 0.75m/s, 35:1 ratio, 80%WC, 40ppm**

39
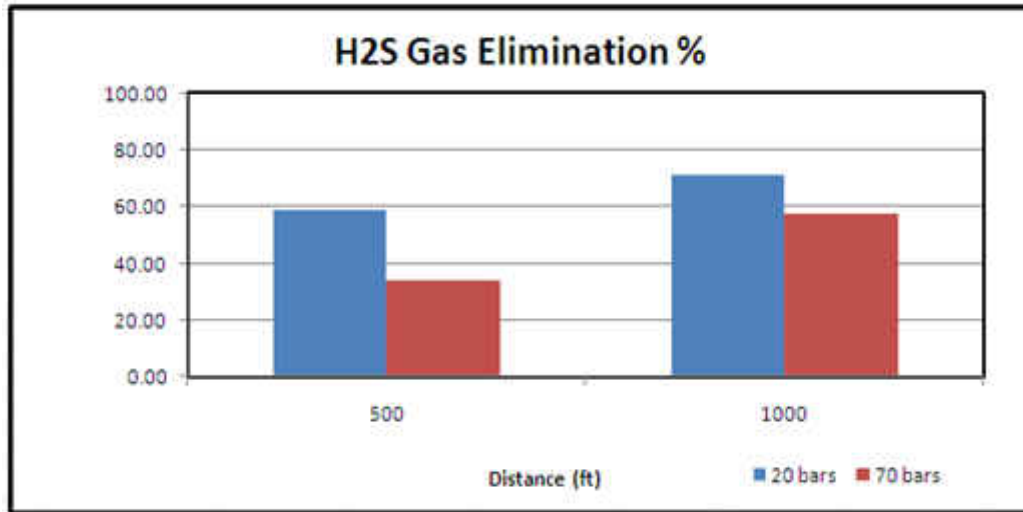
Figure 21: Preliminary Test: Vsl =0.215m/s, Vsg = 0.75m/s, 35:1 ratio, 80%WC, 150ppm

Making the initial H_2S concentration constant for all tests was critical to ensure the same trend is seen for even higher starting concentrations. In Figure 22 the difference between 150ppm and 350ppm starting concentration can be seen. Although this was done at high pressure the same understanding can be made for doing the test at low pressure because shown previously the pressure had little effect on the lower initial concentration and a slightly higher effect at larger initial concentrations. Thus, it can be concluded that the highest initial concentration 350ppm would have a better efficiency at low pressure than shown below. As shown in the Figure 18 and 19 the same trend can be seen here with the lower starting concentration having a better overall efficiency. Also seen is the lower initial concentration value having a larger increase in efficiency with the increase of contact time. Due to these results, it was confirmed that using the 40ppm starting concentration allows for a better chance at higher efficiencies.

40
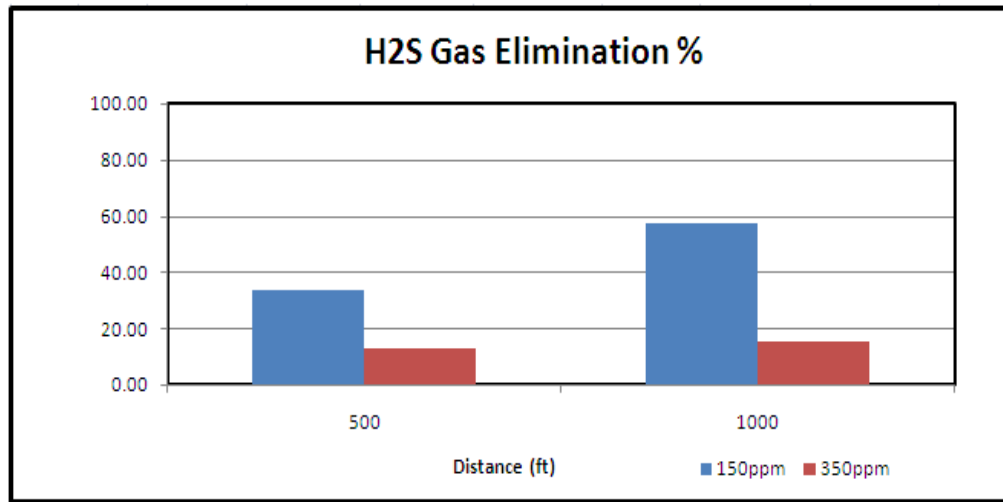
Figure 22: Preliminary Test: Vsl =0.215m/s, Vsg = 0.430m/s, 35:1 ratio, 80%WC, 70bar

<u>Effects of Superficial Liquid Velocity</u>

As mentioned above, a Gas-Alert H_2S monitor with the accuracy of 1ppm was utilized for all experiments conducted. The flow rate was controlled and delivered by a regulator at around atmospheric pressure for 90 seconds. The 500ft and 1000ft sample collectors were both utilized for all testing. After running a series of tests consisting of four superficial gas velocities with one superficial liquid velocity, the system was cleaned with kerosene and water to remove any residual scavenger to prevent memory to the system.

Table 5: Test Matrix

	Initial Parameters					Results at 500ft			Results at 1000ft		
Test #	VSL (m/s)	VSG (m/s)	Pressure (bar)	H2S Mass in Gas Phase (g)	Mass Absorbtion (g)	Gaseous H2S (ppm)	Efficiency (%)	H2S Gas Scrubbed (g)	Gaseous H2S (ppm)	Efficiency (%)	H2S Gas Scrubbed (g)
1	0.215	0.430	19.7	0.053841	1.29	12	70.00	0.037689	4	90.00	0.034997
2	0.214	0.750	20.4	0.05779	1.39	21	47.50	0.02745	12	70.00	0.040453
3	0.216	0.916	19.0	0.065363	1.57	25	37.50	0.024511	21	47.50	0.031048
4	0.215	1.076	19.7	0.10526	0.94	25	26.47	0.027863	22	35.29	0.037151
5	0.322	0.429	21.8	0.057225	1.37	20	50.00	0.028613	26	35.00	0.020029
6	0.344	0.803	19.0	0.052237	1.53	9	72.73	0.03799	10	69.70	0.036408
7	0.323	0.915	19.1	0.076406	1.83	9	77.50	0.059215	4	90.00	0.068765
8	0.323	1.075	20.1	0.040443	1.26	12	61.29	0.024787	5	83.87	0.03392
9	0.429	0.429	19.0	0.058149	1.40	27	32.50	0.018898	23	42.50	0.024713
10	0.431	0.754	19.0	0.106876	1.78	19	52.50	0.05611	15	62.50	0.066797
11	0.430	0.914	21.8	0.070735	1.47	16	65.22	0.046131	7	84.78	0.059971
12	0.430	1.074	21.8	0.059989	1.44	9	77.50	0.046492	7	82.50	0.049491
13	0.536	0.429	19.7	0.057108	0.73	24	35.14	0.020065	23	37.84	0.021608
14	0.538	0.753	19.0	0.062187	1.49	25	37.50	0.02332	17	57.50	0.035757
15	0.537	0.913	19.4	0.093553	2.25	17	57.50	0.053793	18	55.00	0.051454
16	0.537	1.074	19.7	0.062994	0.81	15	61.54	0.038766	13	66.67	0.041996

The test matrix is broken down into three sections. The first section describes all the initial parameters, the second section presents the results obtained at the 500ft location while the third section presents results at the 1000ft location. From these results two important features were examined, the efficiency and the mass absorption in the beginning. These graphs were developed and are shown below.

The first set of testing was at a constant superficial liquid velocity of 0.215m/s. The variables changed were the superficial gas velocity which included 0.43, 0.75, 0.916 and 1.076m/s. The most noticeable trend is that as the superficial gas velocity increased the scavengers efficiency decreased (Fig 23) for both the 500 and 1000ft sample collector. Although the decreasing trend is roughly constant from point to point the greatest drop in efficiency occurred between 0.43m/s and 0.75m/s (~20%) while the smallest was between 0.75m/s – 0.916m/s and 0.916m/s –

1.076m/s (~10%). For all the superficial gas velocities, the 500ft sample collector efficiencies were below that of the 1000ft collector. The greatest difference seen comes at the two lowest gas velocities and the smallest at the two highest gas velocities. This behavior suggests that as the gas velocity increases the longer scavenger contact time has little effect on the efficiency. Since the longer contact time is having little effect on the scavenger it can be concluded that the reaction process is coming to an end. Whereas for the lower gas velocities the scavenger reaction is still taking place and at an even higher contact time it is possible the efficiency could increase. One would reasonably assume that with the decrease in volume of liquid a decrease in the H_2S absorption would be present but Figure 24 shows this is not the case. As the gas velocity increases which correlates to a lower liquid volume a slow increase in mass absorption is seen up to $V_{SG} = 0.916$m/s which then shows the mass absorption decreasing.
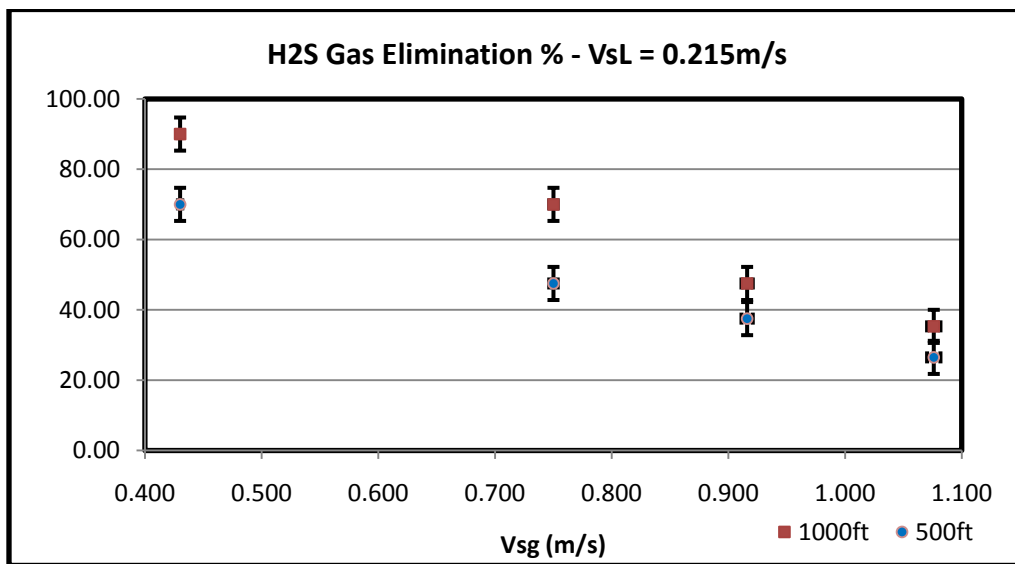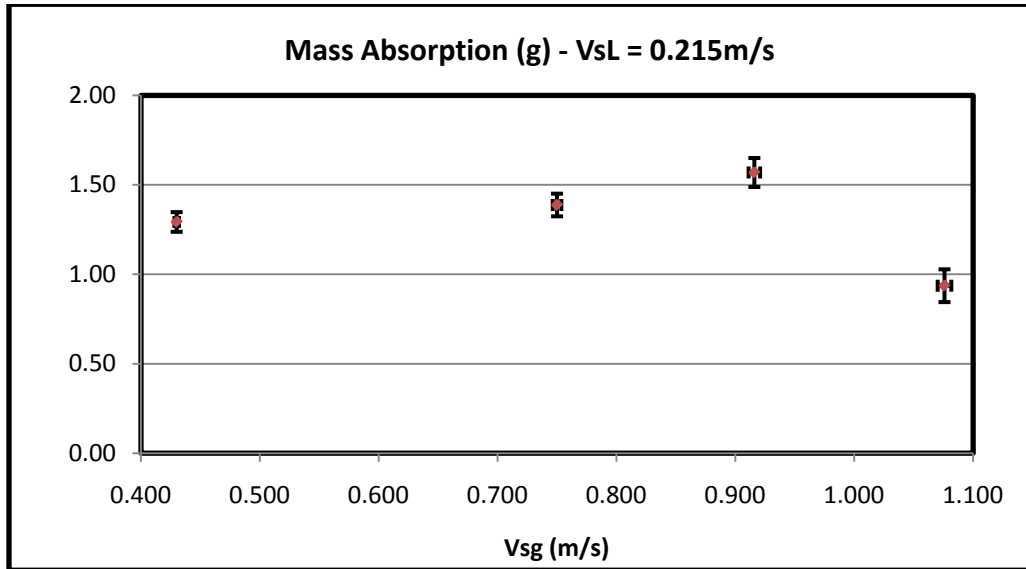

Figure 23: Scrub Efficiency for Vsl = 0.215m/s

43

Figure 24: Mass Absorption at Vsl = 0.215m/s

The next set of testing was conducted at a constant superficial liquid velocity of 0.322m/s. The superficial gas velocities were the same as the previous experimental set. Notice that at the superficial gas velocity of 0.43m/s a minimum efficiency was experienced (~39% at 1000ft, ~50% at 500ft) while the maximum is at 0.916 (~90% at 1000ft, ~80% at 500ft) (Fig 25). The main trend experienced is a steady increase in efficiency until about 0.9m/s gas velocity where it slowly decreases to around 82% and 60 % efficiency for 1000ft and 500ft locations respectively. This deviation in the data trend from the previous data demonstrates a change in the flow characteristics thus causing the mixing of the two liquids to be different ultimately affecting the scavenger's behavior on the reaction with the H_2S. The difference in the trends will be better explained in the liquid volume effects section. Another important aspect to note is that as the gas

44

velocity in this case increases, an increase in the efficiency is seen for longer contact time. It is noticed that the 500ft sample collector produced a higher efficiency than that of the 1000ft sample at the lowest gas velocity. This indicates that the efficiency has reached its peak and has slowly decreased due to the gas that was absorbed into the liquid being released from the highly chaotic flow characteristics. It is also significant to note that the mass absorption follows the same trend as the scrub efficiency of the scavenger, Figure 26.
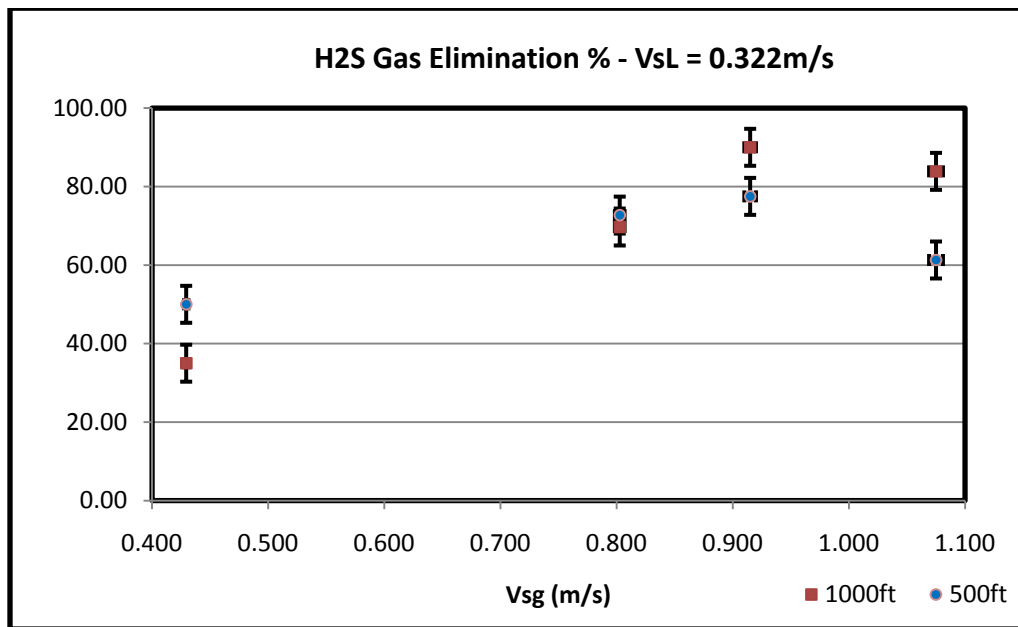

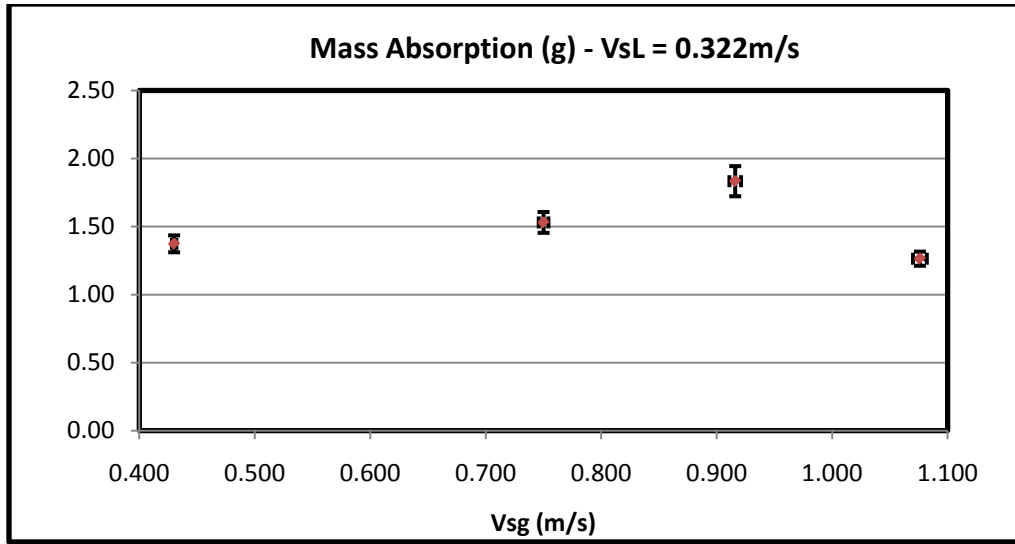**Figure 25: Scrub Efficiency for Vsl = 0.322m/s**

Figure 26: Absorption at Vsl = 0.322m/s

The third part of the testing matrix consisted of setting the superficial liquid velocity to a constant 0.43m/s while changing the superficial gas velocity in the same manner as done in previous tests. From this set of data a reverse affect is seen when compared to the 0.215m/s superficial liquid velocity (Fig 27) for the 500ft location and similar trend as the 0.322m/s liquid velocity for 1000ft location. The most concluding remark for this data set is that the 500ft and 1000ft data marks are roughly the same which suggests that the scavenger's efficiency is not changing with the longer contact time with the exception of the liquid velocity of 0.916m/s. This can either suggest that an outlier is present or something uniquely is happing in the flow characteristics at this particular velocity combination. For this particular test set, the mass absorption had little to do with the gas velocity suggesting that the flow characteristics are nearly the same for all the velocity combinations, Figure 28.
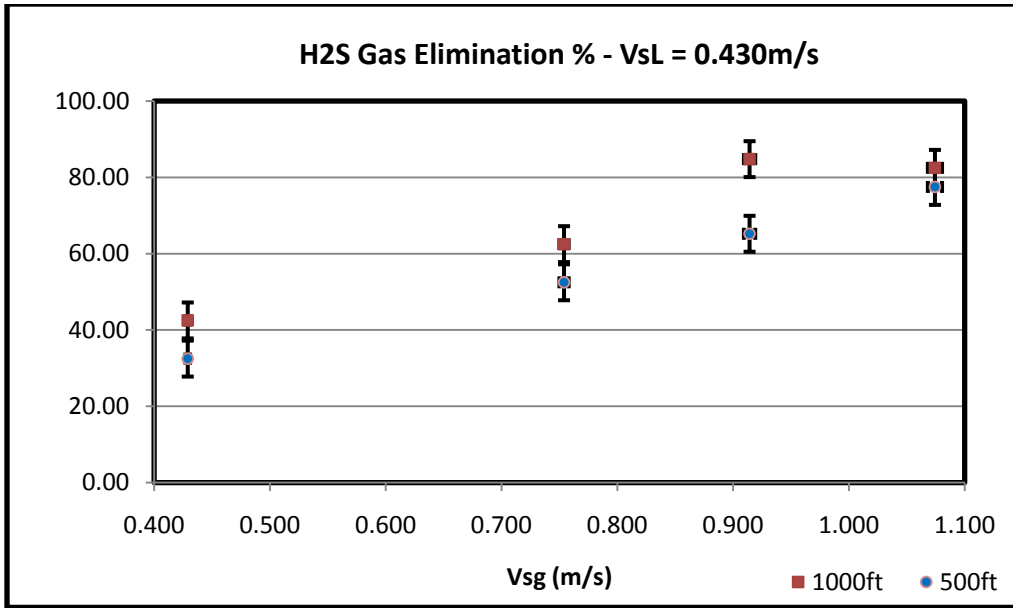
46

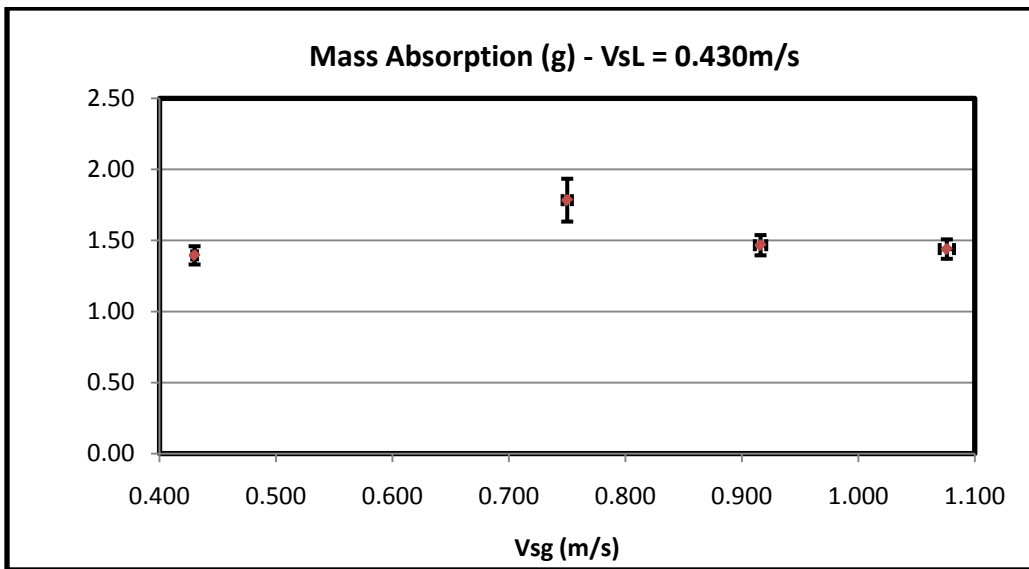**Figure 27: Scrub Efficiency for Vsl = 0.43m/s**

Figure 28: Absorption at Vsl = 0.43m/s

47

The last section of the matrix was to repeat the above set of experiments with a change in superficial liquid velocity to a constant value of 0.537m/s. Unlike the first set of data at 0.215m/s but similar to 0.43m/s, the trend increased as the superficial gas velocity increased (Fig 29), while the maximum efficiency occurred at 1.076m/s (~66%) for both sample collectors and a minimum at 0.43m/s (~37%). The increase in scavenger efficiency from point to point was once again roughly the same but with a smaller value than the previous data (~10%). Overall, the values were roughly the same as set 1, with a difference being a negative slope for set 1 and a positive slope for set 4. The same is seen in this data set as the previous set with both the 500ft and 1000ft sample collectors having roughly the same values with the exception of the liquid velocity of 0.75m/s. This suggest that the scavengers efficiency was not effected much by the longer contact time but more or less by the liquid and gas velocities. Once again this unique value can be suggested as an outlier or a unique occurrence that's happening at the 0.75m/s liquid velocity. Looking at Figure 30 one can observe that the mass absorption bares similar results as the 0.215m/s liquid velocity with the exception of the decrease at the end being more dramatic. It is shown that as the mass absorption increased with increasing gas velocity the efficiency increased, but at the largest gas velocity the efficiency increased while the absorption came down. This means that at this particular point the efficiency is being strongly affected by the flow characteristics rather than the amount of H_2S absorbed into the liquid.
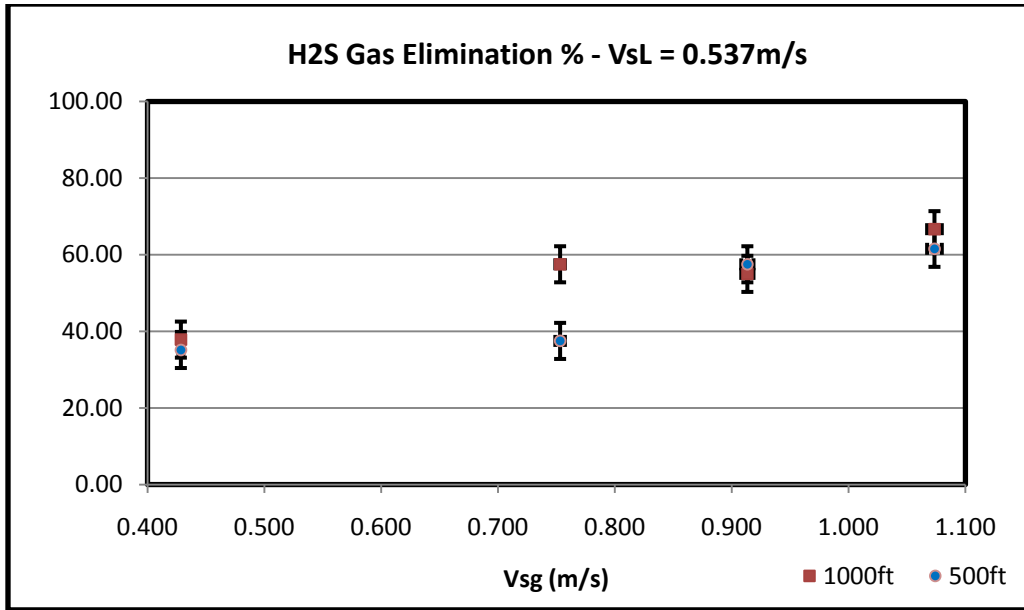
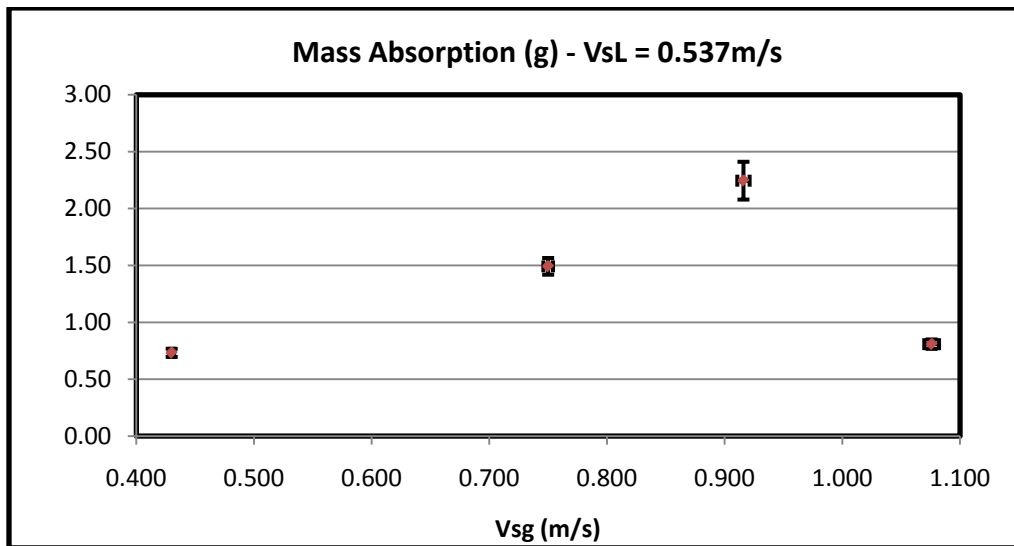**Figure 29: Scrub Efficiency for Vsl = 0.537m/s**

Figure 30: Absorption at Vsl = 0.537m/s

49

Effects of Superficial Gas Velocity

In the figures below the same data was utilized in order to see how the scavenger efficiency changed with an increase in superficial liquid velocity at a given gas velocity. The first couple of figures (31 and 32) display the results at a constant gas velocity of 0.43m/s. These results indicate that as the liquid velocity increases the efficiency decreases to a value of ~35-40% where the efficiency levels off, Figure 31. Also, notice that as the liquid velocity increases the effects of longer contact time diminishes. The only exception to this is the 0.32m/s liquid velocity case where the longer contact time showed a lower efficiency than the shorter contact time. The results indicate that this case is either an outlier or that the scavenger's effects have subsided and liquid absorbed gas has begun to be released into the gas phase again. When comparing this figure to that of the mass absorption graph, Figure 32, it is seen that as the liquid velocity increases so does the mass absorption which correlates to a lower efficiency. At the highest liquid velocity the opposite is seen, the mass absorption decreases dramatically. This occurrence can be explained by the flow characteristics at this particular velocity combination. Within these parameters, the liquid volume is the greatest and thus, the bubbles behind the slug and/or plug is not as chaotic when passing through the channel as the previous ones. As a result, the mixing is not as efficient, which ultimately results in less absorption.
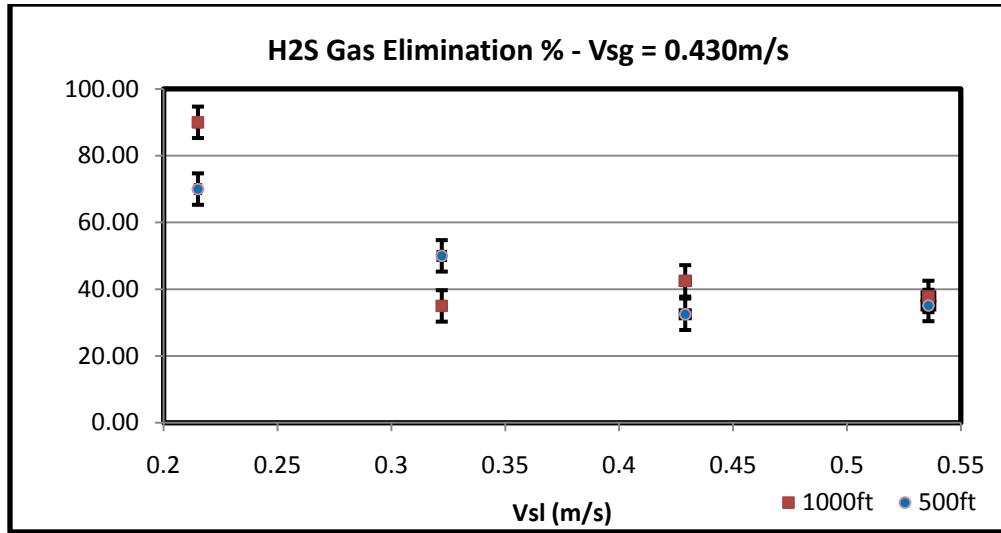
50

Figure 31: Scrub Efficiency for Vsg = 0.430m/s
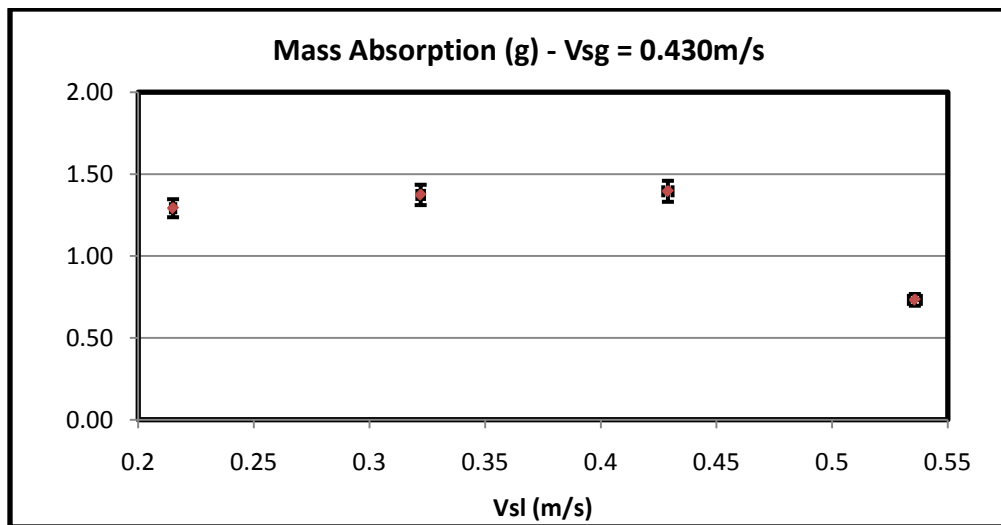
Figure 32: Absorption at Vsg = 0.430m/s

Figure 33 displays the results at a constant gas velocity of 0.75m/s. These results indicate the efficiency behaving like a linear profile for the longer contact time and a parabolic profile for the shorter contact time. Also to notice is that as the liquid velocity increases the effects of longer contact time diminishes at the 0.32m/s liquid velocity but increases again at the higher liquid velocities. When comparing this figure to that of the mass absorption graph, Figure 34 it is seen that the mass absorption profile correlates well with that of the efficiency profiles. The only difference is the profile for the mass absorption is shifted slightly right where its maximum value aligns with 0.43m/s liquid velocity instead of 0.32m/s which correlates to the maximum value for the efficiency profiles. The trend in this graph is completely opposite from the previous graph which will be better explained in the next section.
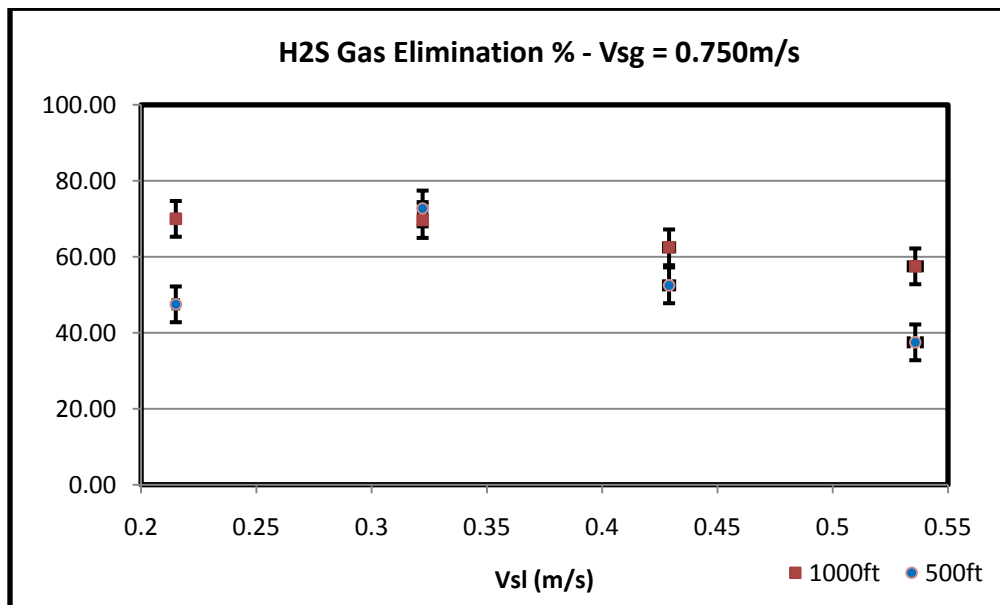
**Figure 33: Scrub Efficiency for Vsg = 0.75m/s**
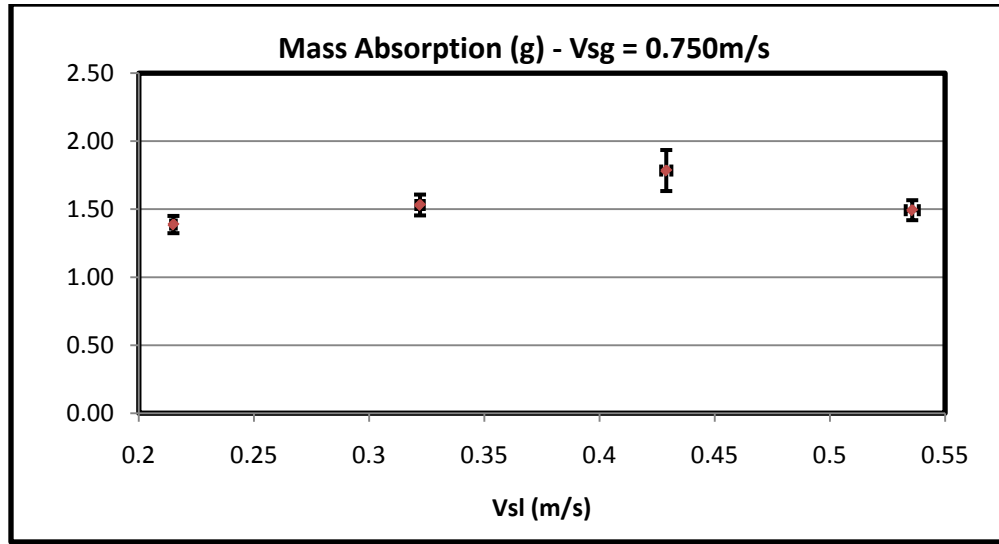
Figure 34: Absorption at Vsg = 0.75m/s

In Figures 35 the results are at a constant gas velocity of 0.916m/s. These results indicate the efficiency behaving like a parabolic profile for both contact times. These results show similar results as those previously shown with the major difference coming from the steepness of the profiles, but with the same maximum value coming at the liquid velocity of 0.32m/s. Notice that as the liquid velocity increases the effects of longer contact time begins to increase to a maximum value at 0.43m/s liquid velocity but diminishes to roughly no effect at the higher liquid velocity. When comparing this figure to that of the mass absorption graph, Figure 36, it is seen that some unique results are happening. The mass absorption profile has an up and down behavior. This indicates that the efficiency is not based on the amount of mass absorption but more or less on the velocity combinations.

53
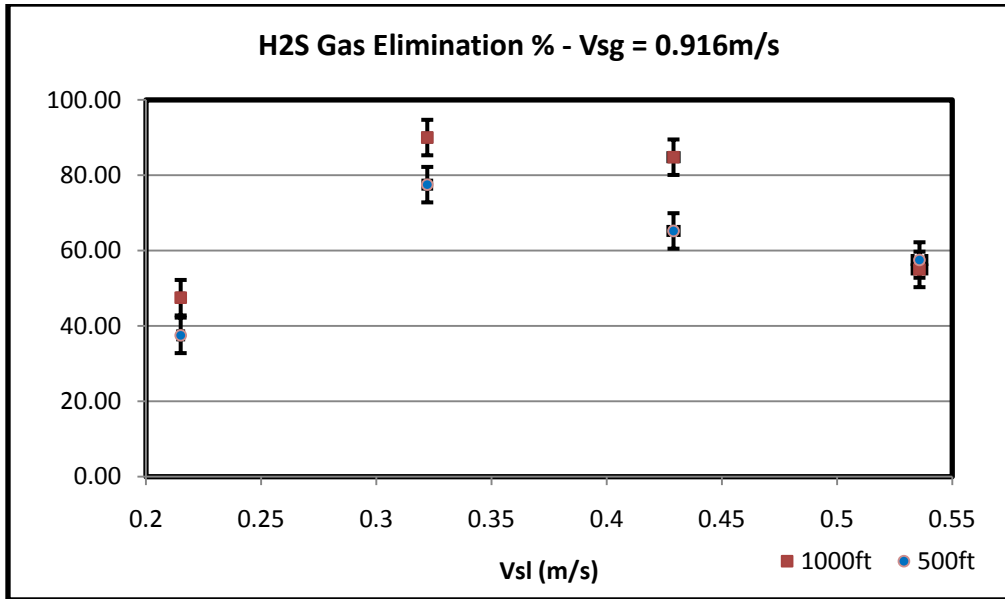
Figure 35: Scrub Efficiency for Vsg = 0.916m/s
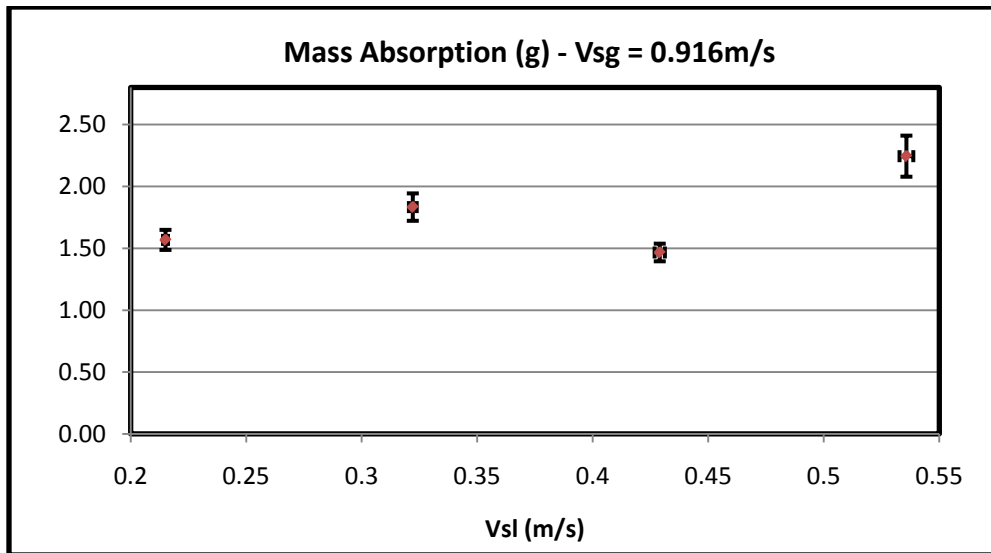
Figure 36: Absorption at Vsg = 0.916m/s

In the next two Figures (37 and 38) the results are at a constant gas velocity of 1.076 m/s. These results indicate the efficiency behaving like a parabolic profile for both contact times. These results show similar results as the two previously shown with the major difference coming from the steepness of the profiles, but with the same maximum value coming at the liquid velocity of 0.32m/s for the longer contact time but at 0.43m/s for the shorter contact time. Notice that as the liquid velocity increases the effects of longer contact time begins to increase to a maximum value at 0.32m/s liquid velocity but diminishes to roughly no effect at the higher liquid velocities. When comparing this figure to that of the mass absorption graph, Figure 38, it is seen that the mass absorption profile correlates well with that of the efficiency profiles for the shorter contact time. The only difference is at the longer contact time where the profile for the mass absorption is shifted slightly right where its maximum value aligning with 0.43m/s liquid velocity instead of 0.32m/s which correlates to the maximum value for the efficiency profiles.
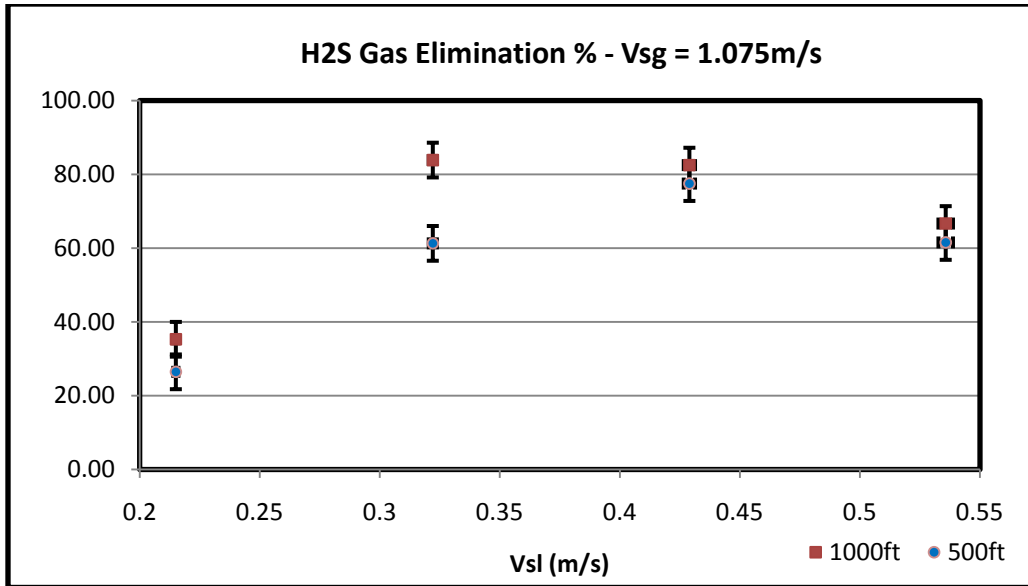
Figure 37: Scrub Efficiency for Vsg= 1.075m/s
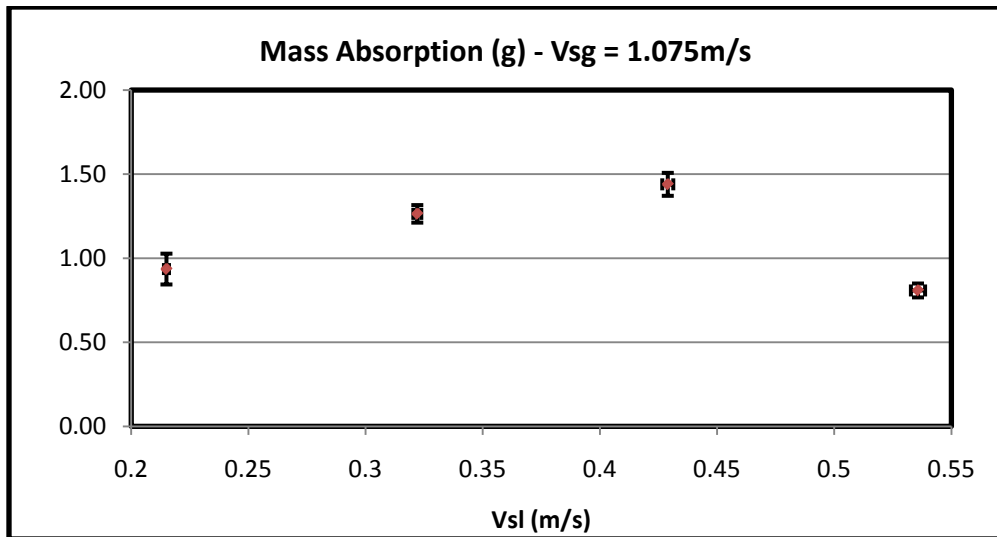
Figure 38: Absorption at Vsg = 1.075m/s

56

Now superimposing all four superficial gas velocities and superficial liquid velocities on to the same graph (Fig 39 and 40) a deeper comparison can be made. Looking at the 0.215m/s superficial liquid velocity, the lower the superficial gas velocity is the higher the scavenger's efficiency becomes while the opposite is seen for the majority of all other liquid velocities for both contact times. The unique characteristic for the 1000ft location is the 0.32 and 0.43m/s liquid velocity which have the 0.916, and 1.076m/s gas velocity close together while the other two liquid velocities are spread apart, Figure 39. This separation is explained by a change in the flow characteristics causing a different form of mixing. Figure 40 is that of the superimposed gas velocities data for the 500ft location. The unique discovery here is like that of the 1000ft collector where some of the superficial gas velocities pair up nicely to each other at certain superficial liquid velocities which indicates a similarity in the flow patterns.
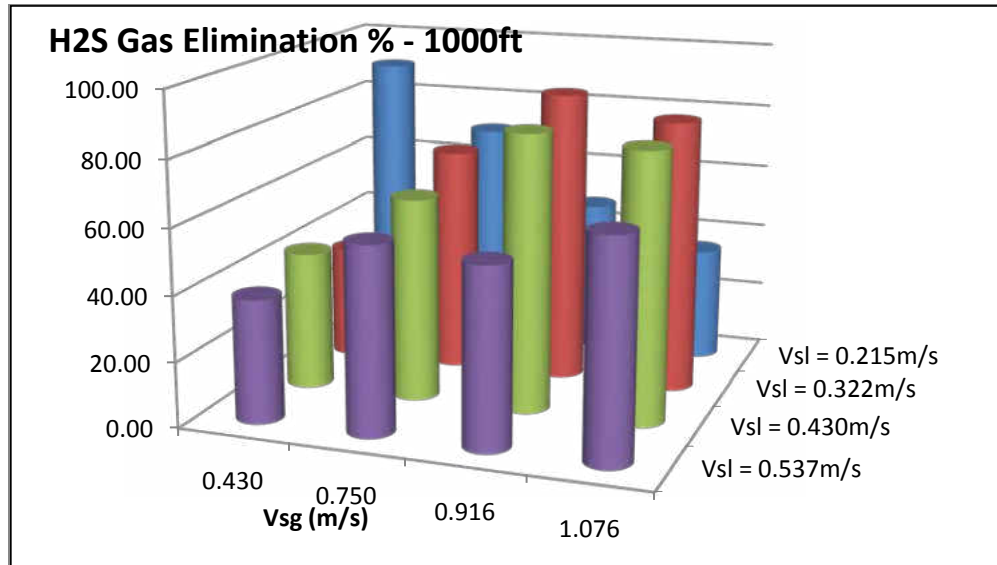
Figure 39: Gas and liquid effects on efficiency at 1000ft

57
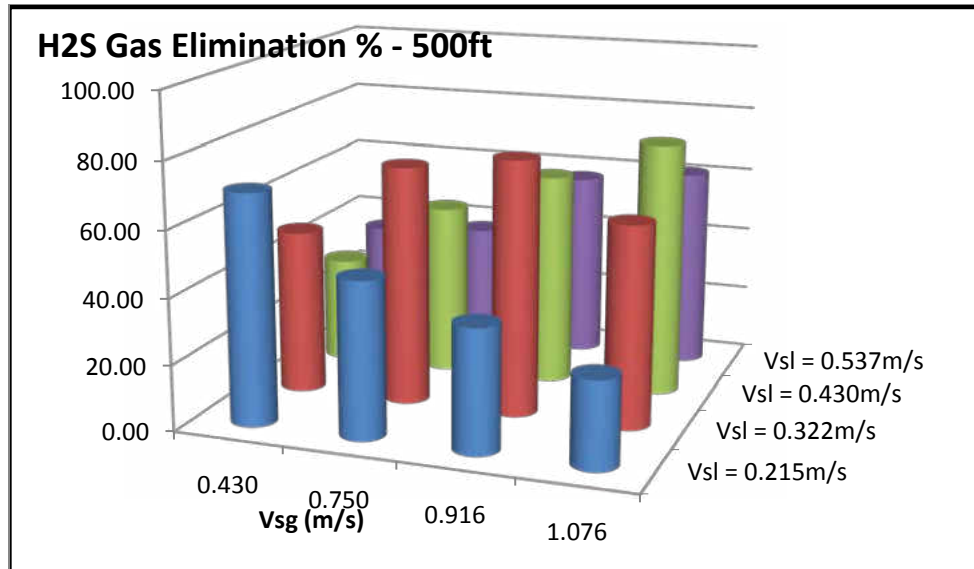
Figure 40: Gas and liquid effects on efficiency at 500ft

Effects of Liquid Volume

Since the multi-phase pump is a progressive cavity pump the volumetric flow rate will always be constant no matter what phase is being pushed through the pump. With this being the case the different velocity combinations were setup by inserting a certain amount of liquid. To help clarify some of the trends expressed above it is important to see how these results are affected by the volume of liquid since this is directly correlated to the velocities. The first set of data that had unique trends was the H_2S mass absorption into the liquid. Figure 41 shows how the mass absorption is affected by the increase in liquid volume. One would think that as the liquid volume increase so should the mass absorption. This would probably be true if the liquid is in a static state verse a moving state. As it can be seen from the graph, the mass absorption in this case really doesn't have any trends with the increase in liquid volume. Although there are some

58

points that are elevated slightly, the majority of the points are in the same region. The same can be said about the total amount of mass of H_2S that is not absorbed by the liquid, Figure 42. With these graphs it is reasonable to say that the mass absorption is not a function of liquid volume in a moving situation but is possibly highly dependent on the flow regime present, and since all test were in the intermittent regime this makes perfect sense for no change to be experienced.
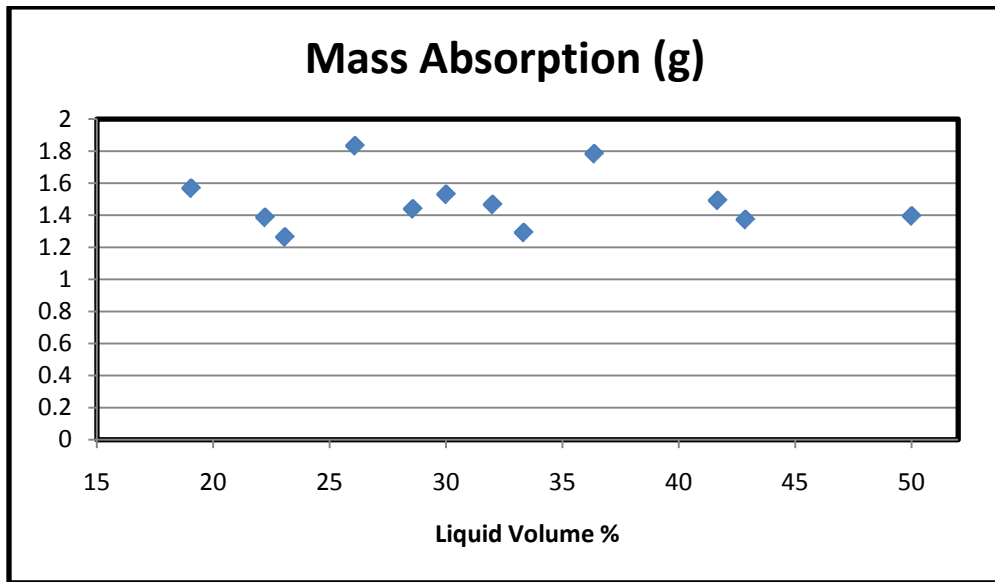
Figure 41: Liquid volume effects on mass absorption
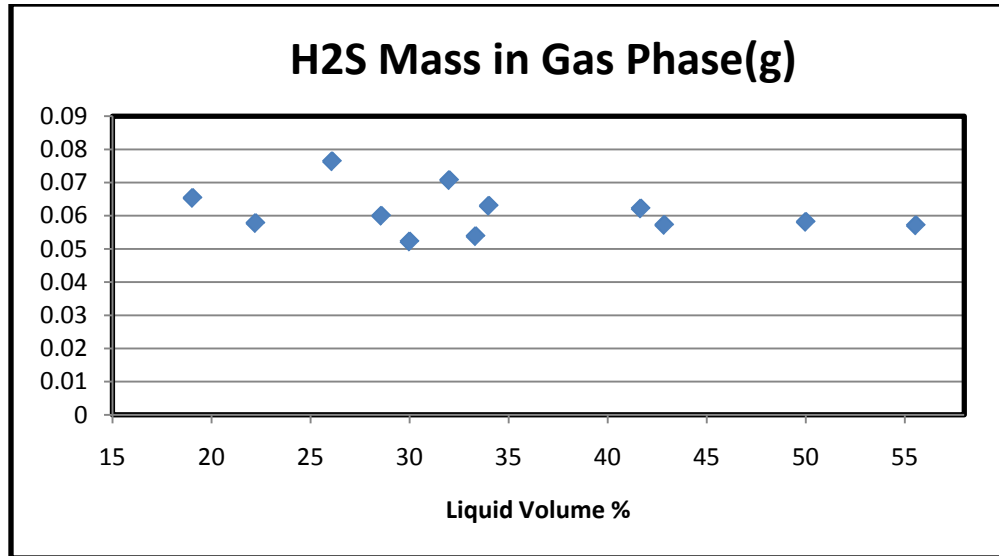
Figure 42: Liquid volume effects on H2S in Gas Phase

It is thought that since the scavenger being utilized reacts with the H_2S absorbed by the liquid and that the more being absorbed due to the greater amount of liquid, a stronger efficiency would be generated. Unfortunately this is not completely true. As seen above, the amount of H_2S in the liquid is not really a function of liquid volume but maybe of the flow regime. Thus, a stronger efficiency is not associated with a higher absorption amount. If this is the case then it is important to understand whether the efficiency is a function of liquid volume. It seems that as the liquid volume increase so does the scavenger's efficiency but up to a certain extent which then decreases in a parabolic manner. This explains why for the first set of data and the later sets are completely opposite of each other. The first set goes from the peak down the left side of parabola and the other sets go from the right side of the parabola to the top of the peak. It is shown that the optimal efficiency lies in the range of 23-33% liquid with≤5% error between the points. Since the mass absorption is not a function of liquid volume the peak also shows where the majority of

60

the H_2S is being removed occurs, which suggest that this is the region where the maximum cost and environment effectiveness takes place. This same trend can be seen at the 500ft location with the only difference being the optimal efficiency level is just a little lower than the 1000ft location which suggest the contact time is having some effect on the scavenger, but at certain locations the contact time is having little to no effect. These trends are indicating something is happing to the flow patterns within this liquid volume range. It has been noticed that within this region the passing of the slug and/or plug causes a highly chaotic mixing behavior behind the slug and/or plug which allows the scavenger to interact with the H_2S more efficiently. After this region, the volume of liquid increases thus causing the slugs and/or plugs passing to have a smoother transition from one another, decreasing the efficiency.
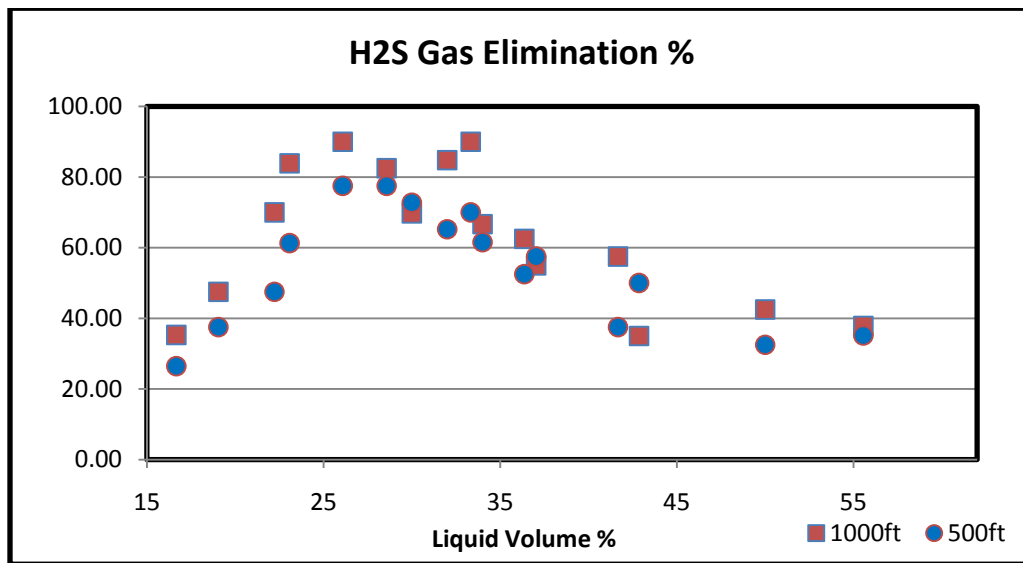
Figure 43: Liquid volume effects on scrubbing efficiency
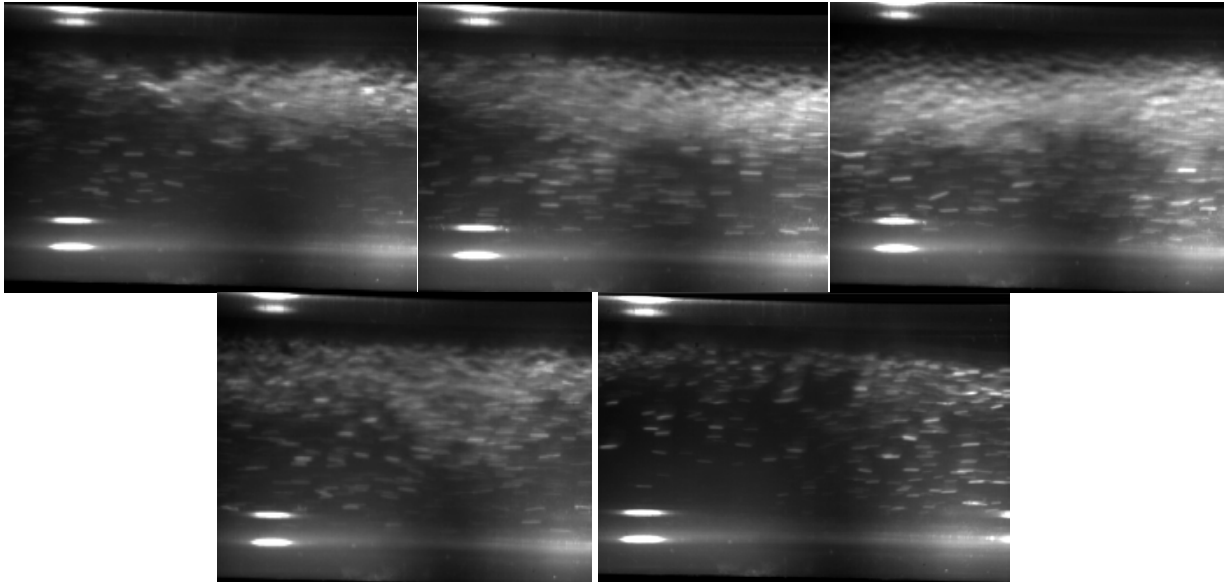
Figure 44: Visualization for different liquid volume: Top - 16%, 23%, 30% respectively: Bottom – 37%, 55%

The next two figures display how much gas is being scrubbed by the scavenger at both contact times. Figure 45 shows a slightly parabolic profile for the lower contact time while Figure 46 shows a smaller parabolic profile at the higher contact time. For the lower contact time it can be seen that the there are clusters around a certain liquid volume while the higher contact time is more dispersed. Both of which show a trend that as the liquid volume increases to a certain point (28-33%) the amount of gas scrubbed increases but as the volume keeps increasing the amount of gas scrubbed decreases. These trends indicate changes to the flow patterns at this liquid volume which was shown and explained in the previous two figures.

62
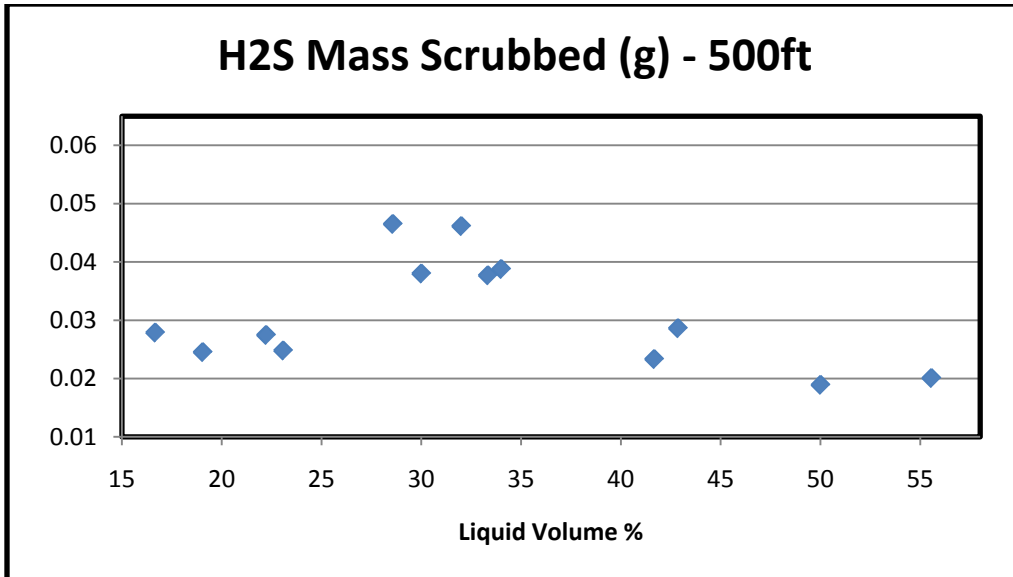
Figure 45: Liquid volume effects on H2S mass scrubbed at 500ft
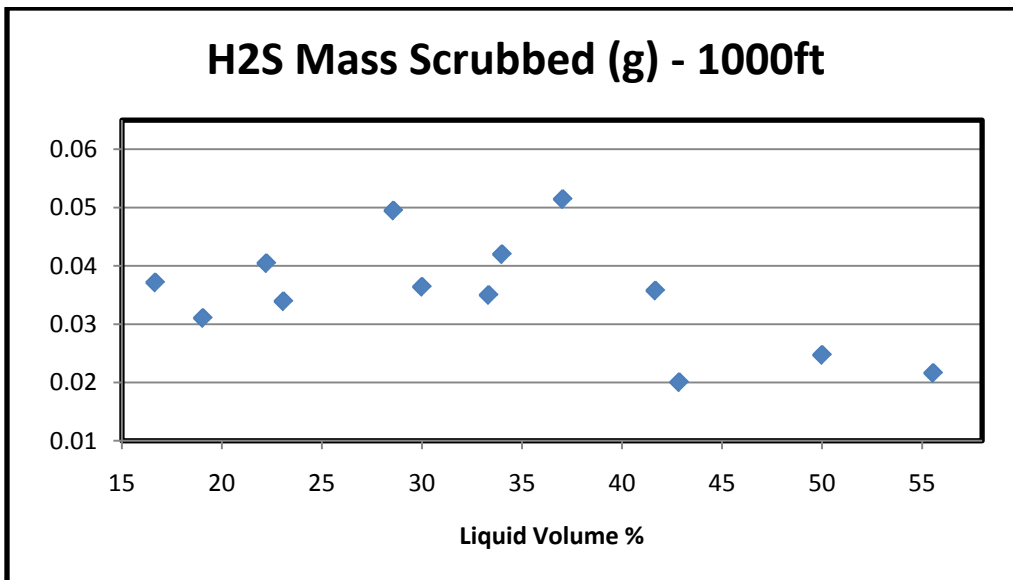
Figure 46: Liquid volume effects on H2S mass scrubbed at 1000ft

63

The last two figures display the amount of gas being scrubbed by the scavenger based on the amount of gas absorbed by the liquid. Figure 47 demonstrates that the mass being scrubbed is not a function of the mass absorbed by the liquids for the lower contact time, while Figure 48 shows the same trend at the higher contact time. Although it can be seen for both contact times that at the end a slight increase in the mass scrubbed is seen for a higher mass absorption. This can be associated with some propagation of error since the majority of the points are showing no real increase in the mass scrubbed for the increase in mass absorption. These trends indicate that the amount of gas scrubbed is not a function of the mass absorption but a function of the velocities which correlate to different flow patterns.
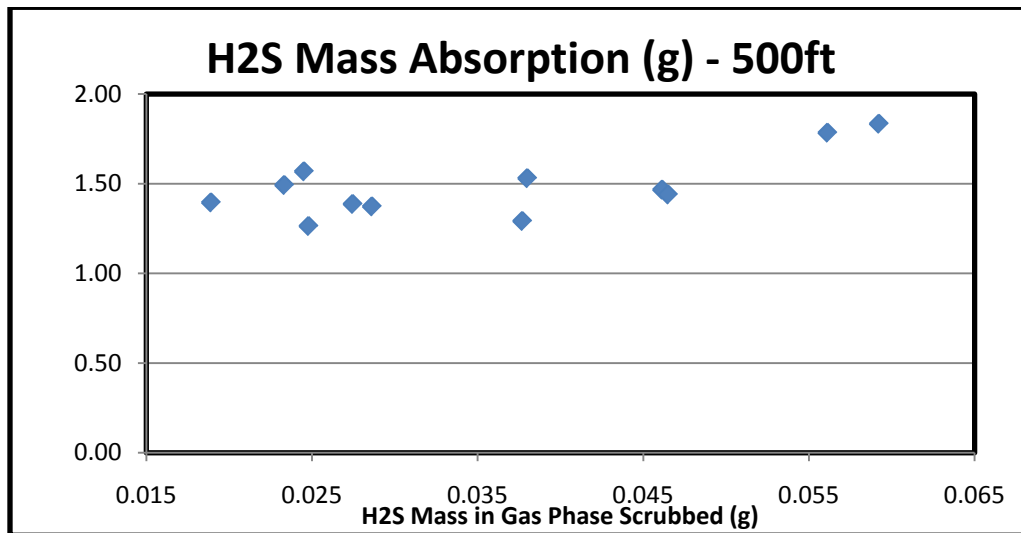
Figure 47: The effects of H2S absorption on H2S gas scrubbed at 500ft

64
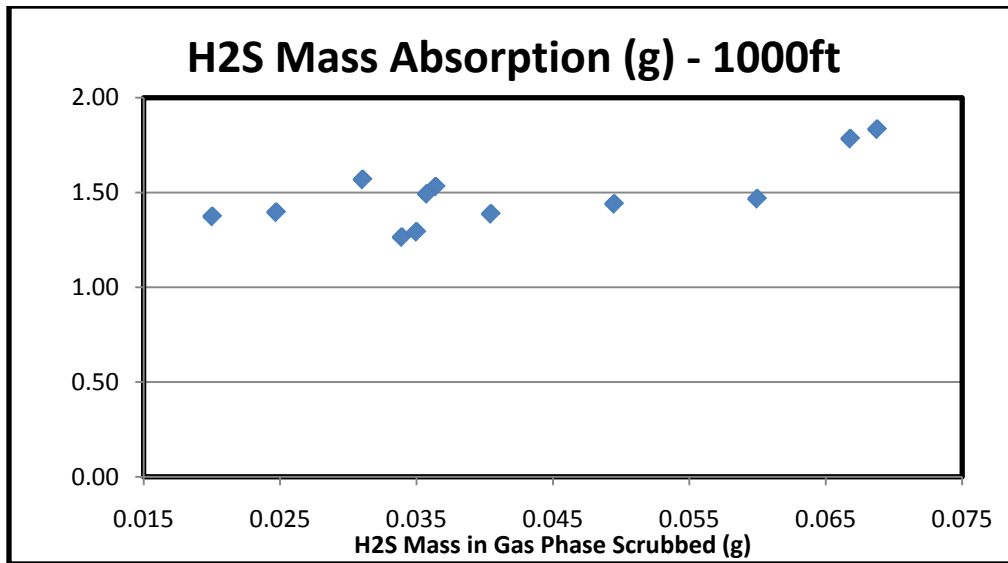
Figure 48: The effects of H2S absorption on H2S gas scrubbed at 1000ft

<u>Pressure and Location Effects for Flow Regime</u>

The second experimental study consisted of more than one hundred different liquid and gas velocity combinations at both 5 and 10bars. These combinations ranged from 0.1 – 2m/s liquid velocity to 0.03 – 2m/s gas velocity. Since the water cut was 80% (brine to oil ratio) for the scavenger loop which is mostly brine it was assumed that a good comparison and understanding of what is happening in the scavenger loop could be made if 100% brine is put into the visualization loop. Within these experiments it was noticed that most of the traditional flow regimes seen at atmosphere was experienced at higher pressures, elongated bubbles, stratified, intermittent (slug, plug, slug/dispersed), and dispersed. Since the probability of annular or mist flows is low in the real world situations, it was not subjected to testing. The two figures below, Figures 49 and 50 are the test runs at 5 and 10bars respectively. Since the loop was a closed loop

65

it was hard to run tests at atmosphere pressure to validate the results obtained. In the figures, two lines are drawn; the solid black line is based on theory by Mandhane and the short dashed line done experimentally by Dukler. Since the majority of data collected match within the region created by Dukler, it was concluded that the results were reasonably correct. The longer dashed lines are drawn based on experiments run for this study which represent the transition between one flow regime to the other. While they are based on the data collected, it should be noted that only a small amount of data was available. The transition line for annular flow was interpolated from the data and was also based on the Mandhane and Dukler transition line. When comparing the three lines together it is seen that little change is experienced for the intermittent regime along the gas velocity scale as the pressure increases, but a big difference is seen in the liquid velocity scale where the stratified and dispersed regime increase causing a collapse of area in the intermittent regime. This suggests that if the pressure was to increase higher a possibility of not having an intermittent regime is possible.
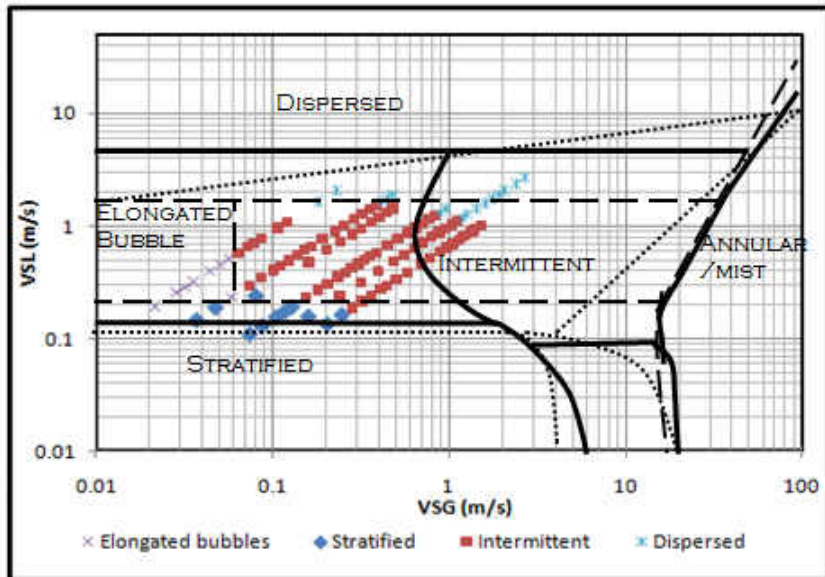
Figure 49: Flow Regime map at 5 bars
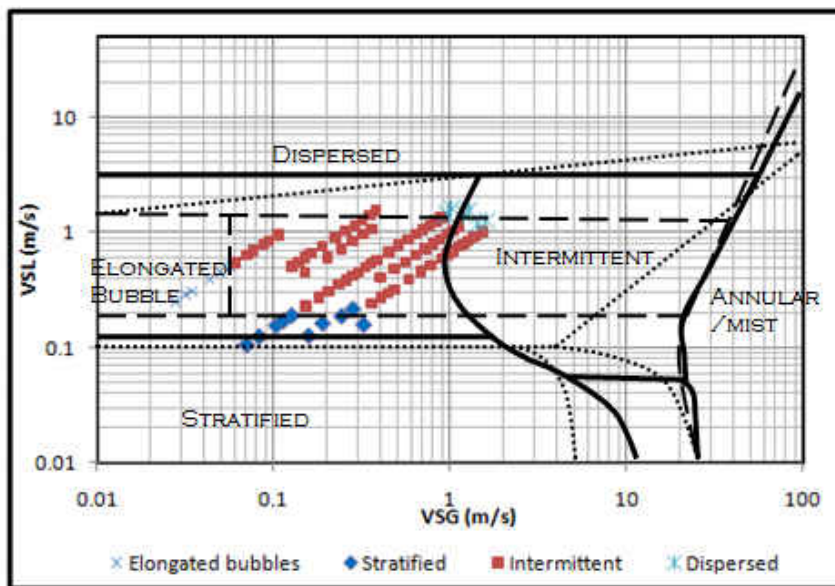
Figure 50: Flow Regime map at 10 bars

Figure 51 and 52 consist of a few case studies that show how the change in pressure is truly affecting the flow characteristics. The top and bottom rows are at two different velocity combinations (intermittent regime) and the columns go from left to right for the increase in pressure. It is shown in both figures that as the pressure increase the bubble formation behind the slug increase in volume (the amount of bubbles) and decrease in size causing a film across the top of the liquid. This indicates a possible shift in the transition between one flow regime and another. Although this is not seen directly, the two figures above it strongly indicates that if the pressure was at a high enough difference a significant change would be experienced with the transition lines possibly making the intermittent regime to vanish. This allows better understanding of the flow characteristics the scavenger would be experiencing under different oil reservoir pressures. With the increase in bubble formation on the surface of the liquid behind these slugs, it is suggested that if the pressure was to increase further, less contact with the scavenger would be made due the scavenger's density being heavier than water. This would ultimately produce a possible lower efficiency, which is shown in the preliminary results. If this is the case then a higher concentration of scavenger would be needed to bring the H_2S down to a safe level.
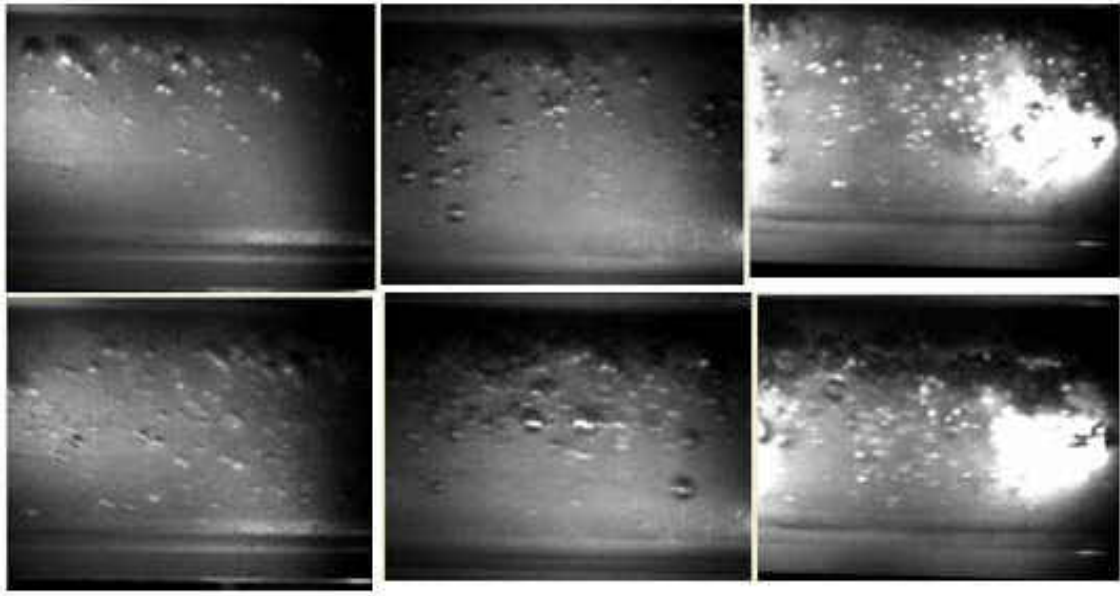
Figure 51: Visualization comparison at 25ft, Left column 5bars, Middle column 10bars, Right column 20bars: Top row Vsl=0.654m/s, Vsg=0.163; Bottom row Vsl=0.894m/s, Vsg=0.224
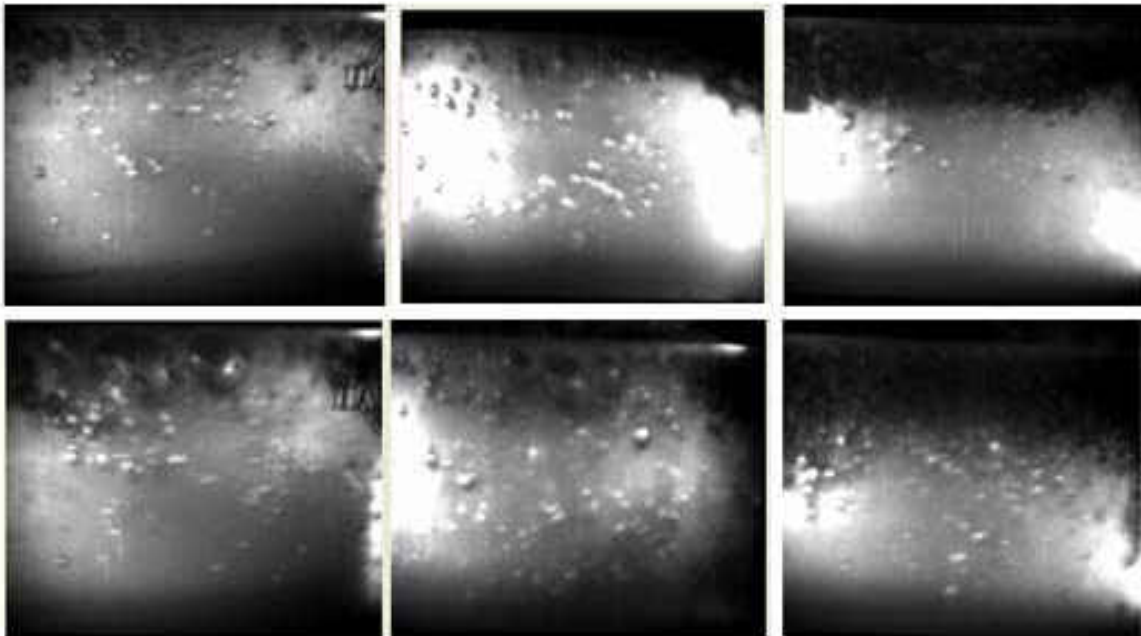
Figure 52: Visualization comparison at 100ft, Left column 5bars, Middle column 10bars, Right column 20bars: Top row Vsl=0.654m/s, Vsg=0.163; Bottom row Vsl=0.894m/s, Vsg=0.224

69

Another concept that needed further exploration was how the increase in distance affects the flow characteristics, which correlates to the scavenger contact time. Although multiphase flow is really never a steady flow, since the system was a closed loop a semi-steady flow was assumed. With this as a comparison, the hundred foot location could be looked at without finding the same differential volume of liquid that passes through the 100ft section as did the 25ft location. Figure 53 shows a few case scenarios of what happens at a further distance along the pipe at 5bars. Just like in the previous figures these cases were looked at in the intermittent flow regime which is the same regime which correlates to the setup one. Within the figure it can easily be seen that as the distance increased the bubbles that accompany the bypass of the slug increase in volume (amount of bubbles present) and size. This suggests that if an even longer distance was considered an even more dramatic effect could be seen. Relating this to the scavenger efficiency shows why the scavenger efficiency increased with increased distance between the two sample collectors. Looking at this increase in bubble volume compared to the one experienced for the increase in pressure, a concluding difference is made. For the increase in pressure, a film of bubbles forms at the top of the liquid where as at the different locations the bubble count and size in the flow increase. Since the scavenger efficiency increases as the distance increased an indication that the enlargement of the bubble volume causes more contact with the scavenger is concluded.
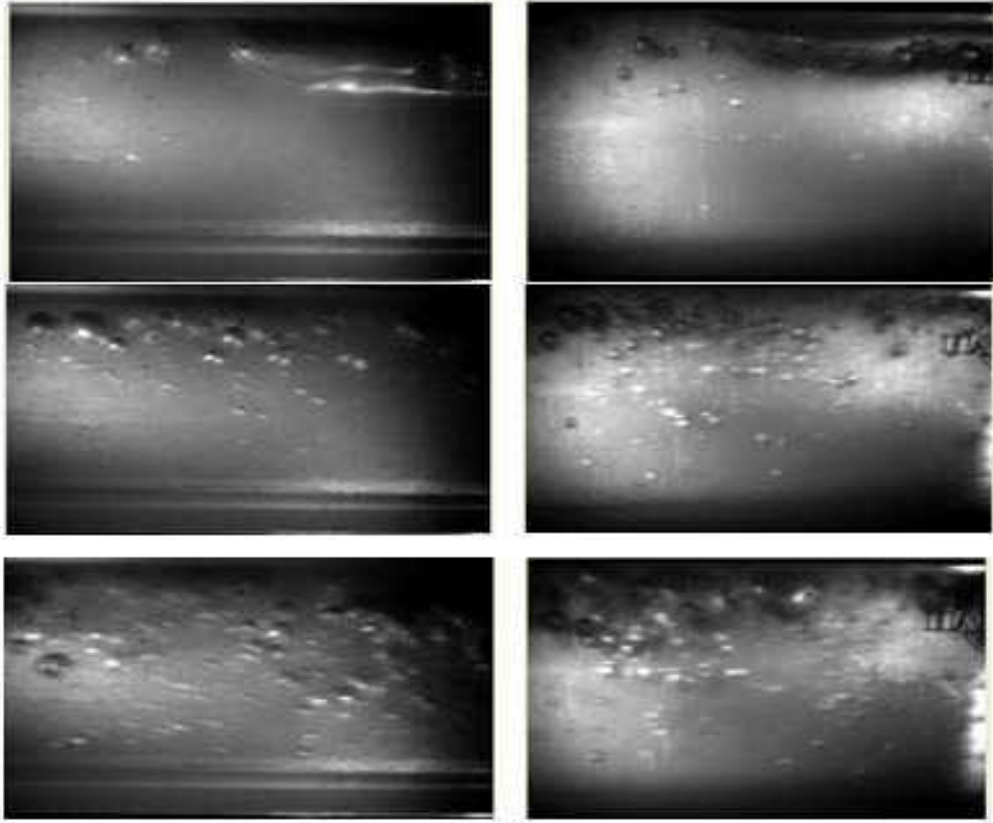
Figure 53: Visualization comparison 5 bars, Left column 25ft, Right column 100ft:Top row Vsl=0.495m/s, Vsg=0.124; Middle row Vsl=0.654m/s, Vsg=0.163; Bottom row Vsl=0.894m/s, Vsg=0.224

CHAPTER FIVE: CONCLUSION

A high pressure closed loop was designed and fabricated to determine the influence of gas, liquid velocities and liquid volume on the H_2S scavenger efficiency. All experiments were conducted in this high pressure loop at 20 bars in room temperature with a thousand feet of coiled tubing to simulate the horizontal section of the pipeline that runs along the ocean floor from the reservoir. The oil utilized was from the Petrobras oilfields. Due to the high complexity of multiphase flow and the unknown scavenger behavior with these flows it is of great importance to understand how the liquid and gas velocities affect not only the scavenger's efficiency, but also the H_2S absorption into the liquid which may or may not have an effect on the efficiency. The following conclusions may be drawn from the experiments in the test loop as well as a 100 ft simulation flow loop which was fabricated for flow visualization.

- This study showed that all data points covered the range up to the intermittent regime (i.e., large slugs and churn-turbulent but not in the wavy annular regime). A maximum H_2S removal efficiency of 80% to90% was obtained when the liquid volume present in the pipe line is between 23-33%. It is hypothesized that when the liquid volume percentage in the pipe is low, large slugs and plugs pass, creating a higher probability for scavenger gas interaction. Thus the maximum efficiency occurs only in the intermittent regime.

- During the experimentation the H_2S mass absorption into the liquid was found to have an equal dependency on the increase of both gas and liquid velocities indicating that the liquid volume had no major effect on the absorption. This was caused by the flow

72

characteristics oscillating from smooth bubble formation to chaotic formation behind the slug and/or plug with the peak efficiency occurring near the middle of the test range. Since mass absorption is roughly constant for all liquid volumes and the efficiency of H_2S removal is maximum at low liquid volumes, the use of scavenger can be optimized for the maximum efficiency. This could cut costs and protect the environment.

- For majority of the tests, maximum scavenger efficiency occurs at 1000 ft (the longer scavenger contact time) due to maximum contact.. The increase in bubble size as the distance increased and the longer time the gas was exposed to the scavenger are thought to be the major influencing factors for this change in H_2S removal from the system at the two locations.

- As the pressure increases the transition from one flow regime to another shifts slightly, mainly shrinking the intermittent regime. The reason for this shrinkage comes from the bubbles decreasing in size and creating a bubble film on top of the liquid surface allowing for an earlier transition from intermittent to dispersed flow as the pressure increases. This can be subjected to further shrinkage in the intermittent flow regime if pressure is incresed even higher until this regime disappears. This may indicate that the H_2S removal efficiency can decrease when the system pressure is increased.

73

APPENDIX A. SCAVENGER SYSTEM OPERATION CHECKLIST

<u>A: Safety Revision</u>

1. Make sure no pressure is inside the loop
2. Make sure all valves are closed except valve 27 and valve 16

<u>B: Fluids Input</u>

Mixing Water Cut Percentage:

1. Open valve 5
2. Open valve 6
3. Open valve 10
4. Open valve 7
5. Open valve 8
6. Open valve 9
7. Turn pump #2 on
8. Let run for 20 minutes

Inputting Desired Liquid:

1. Connect air hose to Pump #3
2. Turn Pump #2 off
3. Close valve 5
4. Close valve 6
5. Close valve 7
6. Close valve 8
7. Close valve 9
8. Close valve 10
9. Turn air compressor on to 40psi delivery pressure
10. Open valve 55
11. Deliver nitrogen to Multi-Phase pump to create a seal
12. Turn Multi-Phase pump on to 15rpm
13. Run for necessary time to reach the liquid volume needed for test (see pump 2 calibration)
14. Turn compressor off
15. Close valve 55

75

Inputting Desired Gas:

1. Open valve 15
2. Input required pressure of Hydrogen Sulfide
3. Close valve 15
4. Open valve 14
5. Input required pressure of Nitrogen
6. Close valve 14
7. Let mix by turning pump at a RPM value to reach required superficial velocities
8. Let mix for 20 minutes
9. Turn Multi-Phase pump off
10. Let settle for 5 minutes
11. Get Reading
12. Repeat process until desired concentration of Hydrogen Sulfide and Pressure is achieved

C: H$_2$S Concentration Reading

1. Turn Multi-Phase pump off
2. Let settle for 5 minutes
3. Make sure all valves are closed
4. Open valve 61
5. Open valve 62
6. Open valve 21
7. Close valve 21
8. Open valve 66
9. Open valve 65
10. Open valve 23
11. Get reading from Regulator 5 for roughly 3 minutes
12. Close valve 23
13. Close valve 65
14. Close valve 66
15. Close valve 61
16. Close valve 62
17. Input Hydrogen Sulfide or Nitrogen according to the Concentration reading

1. Make sure all valves are closed
2. Gather the required amount of scavenger
3. Add roughly half the total volume of scavenger of water
4. Open valve 68
5. Pour scavenger into holding container
6. Close valve 68

E: Sample Collecting

1. With Stopwatch ready and Multi-Pump set
2. Open valve 67 and turn timer on
3. At required time open valve 17
4. Close valve 17, within a few seconds
5. Open valve 61
6. At required time open valve 21
7. Close valve 21
8. Close valve 61
9. Open valve 62
10. At required time open valve 21
11. Close valve 21
12. Close valve 62
13. Open valve 63
14. At required time open valve 21
15. Close valve 21
16. Close valve 63
17. At required time open valve 25
18. Close valve 25

Determining Concentration Reading:

1. Open valve 19 very slowly
2. Deliver 1psi to sensor from regulator 4 for 2 minutes
3. Close valve 19
4. Open valve 64
5. Open valve 23 slowly
6. Flow 1psi to sensor from regulator 5 for 2 minutes
7. Close valve 23
8. Close valve 64
9. Open valve 65

77

10. Open valve 23 slowly
11. Flow 1 psi to sensor from regulator 5 for 2 minutes
12. Close valve 23
13. Close valve 65
14. Open valve 66
15. Open valve 23 slowly
16. Flow 1psi to sensor from regulator 5 for 2 minutes
17. Close valve 23
18. Close valve 66
19. Open valve 23 slowly
20. Flow 1psi to sensor from regulator 5 for 2 minutes
21. Close valve 28

<u>F: System Cleaning</u>

Purging the Loop:

1. Turn Multi-Phase to 45rpm
2. Open valve 34
3. Open valve 36 slowly
4. Once noise has stopped
5. Close valve 36
6. Open valve 42 half way
7. Open valve 46 half way
8. Once noise stops
9. Close valve 43
10. Close valve 46
11. Open valve 50
12. Reopen valve 36
13. Once noise has stopped
14. Close valve 50
15. Close valve 36
16. Open valve 43
17. Open valve 46
18. Once noise has stopped
19. Close valve 43
20. Close valve 46
21. Open valve 50
22. Repeat until pressure in loop is under 100psi
23. Turn Multi-Phase pump off
24. Continue purging process until completely empty

78

Cleaning the Loop:

1. Make sure all valves except for valves 27 are closed
2. Connect air hose to pump #5
3. Open valve 59
4. Turn air compressor to 40psi delivery rate
5. Insert 2 gallons of Kerosene
6. Insert 10 gallons of water
7. Turn pump 5 off by compressor
8. Close valve 59
9. Open valve 55
10. Add nitrogen to 30psi
11. Turn Multi-Phase pump to 45rpm
12. Let run for 20 minutes
13. Turn Multi-Phase pump off
14. Purge the loop as stated above
15. Open valve 59
16. Turn pump 5 on
17. Add 5 gallons of water
18. Turn Pump 5 off
19. Add nitrogen to 30psi
20. Turn Multi-Phase onto 45rpm
21. Run for 20 minutes
22. Turn Multi-Phase pump off
23. Purge Loop

APPENDIX B. VISULAIZATION SYSTEM OPERATION CHECKLIST

<u>A: Safety Revision</u>

1. Make sure no pressure is inside the loop
2. Make sure all valves are closed except valve and valve

<u>B: Fluids Input</u>

Inputting Desired Liquid:

1. Connect air hose to Pump #1
2. Close valve off leading to scavenger system
3. Open valve leading to visualization system
4. Open valve 5
5. Open valve 1
6. Turn air compressor on to 40psi delivery pressure
7. Deliver nitrogen to Multi-Phase pump to create a seal
8. Turn Multi-Phase pump on to 15rpm
9. Run for necessary time to reach the liquid volume needed for test
10. Turn compressor off
11. Close valve 55 from scavenger loop

Inputting Desired Gas:

1. Open valve 2
2. Input required pressure of Nitrogen
3. Close valve 2
4. Let mix by turning pump at a RPM value to reach required superficial velocities
5. Let mix for 20 minutes
6. Turn camera on to get required pictures.
7. Repeat process for other superficial velocities

<u>C: System Cleaning</u>

Purging the Loop:

25. Turn Multi-Phase off
26. Close valve 1
27. Close valve 5
28. Open valve 4 slowly

81

29. When noise has stopped close valve 4
30. Open valve 1 half way
31. Open valve 4 half way
32. Once noise stops
33. Close valve 1
34. Close valve 4
35. Open valve 5
36. Reopen valve 4
37. Once noise has stopped
38. Close valve 5
39. Close valve 4
40. Open valve 1
41. Open valve 4
42. Open valve 5 half way
43. Open valve 17 from scavenger system
44. Turn on Nitrogen regulator to low input
45. Turn Multi-Phase pump on to low rpm
46. Continue until all liquid is out.
47. Turn off Nitrogen tank
48. Close valve 17 from scavenger system
49. Close valve 5
50. Close valve 1
51. Close valve 4

Cleaning the Loop:

24. Make sure all valves except for valves 5 and 1 are closed
25. Connect air hose to pump #5 from scavenger system
26. Open valve 59 from scavenger system
27. Open valve leading to visualization system
28. Close valve leading to scavenger system
29. Turn air compressor to 40psi delivery rate
30. Insert 2 gallons of Kerosene
31. Insert 3 gallons of water
32. Turn pump 5 off by compressor
33. Close valve 59 from scavenger system
34. Open valve 55 from scavenger system
35. Add nitrogen to 30psi
36. Turn Multi-Phase pump to 45rpm
37. Let run for 20 minutes
38. Turn Multi-Phase pump off
39. Purge the loop as stated above
40. Open valve 59 from scavenger system

41. Turn pump 5 on from scavenger system
42. Add 5 gallons of water
43. Turn Pump 5 off
44. Add nitrogen to 30psi
45. Turn Multi-Phase onto 45rpm
46. Run for 20 minutes
47. Turn Multi-Phase pump off
48. Purge Loop as stated above

APPENDIX C. SAFETY, HEALTH AND ENVIROMENT

With the presence of H$_2$S and the scavenger loop being so large the entire rig was built in a hanger building with two bay doors. One in the front and one in the side rear which remains open at all times when the experiment is being conducted, see figure below. To promote even more safety there are two constantly blowing industrial size mechanic fans that are facing the testing area. This helps rid the area of any possible leakage of H$_2$S. To ensure the individual safety of the scavenger systems operators it is required that each wear a 3M 6100 series respirator mask and a hand held H$_2$S monitor on their side. These respirators have cartridges that are changeable roughly every three months and are designed to stop the passing of H$_2$S levels less than 200ppm.
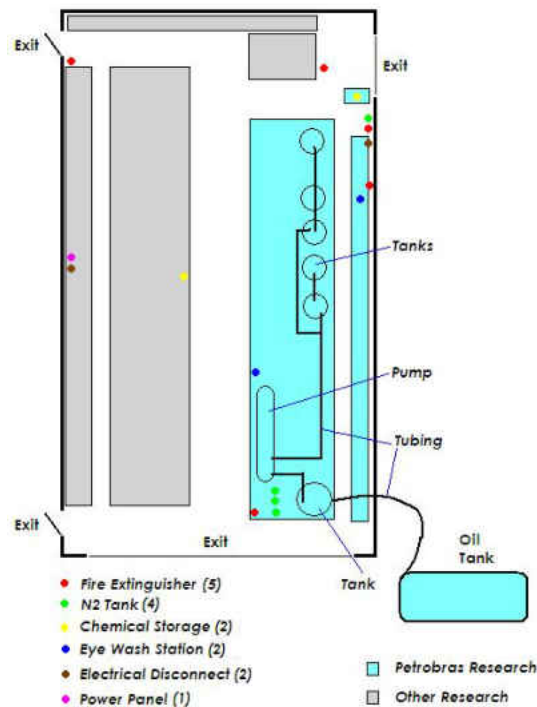

Figure 54: Location of important equipment

As for the visualization system the safety precautions are not as strict. The system has only one safety hazard which is high pressure (20bars). With that in mind when operating this system operators must wear safety goggles for eye protection.

APPENDIX D. ERROR PROPAGATION AND UNCERTAINTY

To find the uncertainty of the liquid volume placed into the loop the error propagation equation is utilized. The uncertainty changes for every test due to the change of volume for every test. They are tabulated in the table below.

1. $U_{Liq,vol} = \sqrt{(\frac{dQ}{dV} U_{pump,vol})^2 + (\frac{dQ}{dt} U_t)^2}$

with

$Q(\frac{gal}{s}) = \frac{Volume}{time}$

$\frac{dQ}{dV} = \frac{1}{t}$

$\frac{dQ}{dt} = -\frac{V}{t^2}$

and $U_{pump,vol} = 0.137$ from calibration curve and $U_t = 0.15$

The same approach was used to calculate the uncertainty value for liquid velocity, water cut %, and mass absorption. The results are in the Table below.

2. $U_{Liq,vel} = \sqrt{(V_L U_L)^2 + (V_{Liq,vol} U_{Liq,vol})^2}$

with V_L is the total superficial velocity, $U_L = 0.0037$ from the pump calibration curve, and $V_{Liq,vol}$ and $U_{Liq,vol}$ are from the previous calculation.

3. $U_{wc\%} = \sqrt{(LU_L)^2 + (WU_w)^2 + (HU_H)^2}$

88

with L, W, H is the length, width, and height of the storage tank that hold the water cut%. U_L, U_w, and U_H are the uncertainty of the measure equipment, $\frac{0.125}{12} = 0.0104$.

4. $U_{H_2S} = \sqrt{(\frac{dm}{dx}U_x)^2 + (\frac{dm}{dP}U_P)^2}$

with

$$m_{H_2S} = \frac{V_{SG}}{V_{SL} + V_{SG}} \times 0.0234(m^3\,{}^{Kg}/_{KJ})P_{tot}\,x_{H_2S}$$

$$\frac{dm}{dx} = \frac{V_{SG}}{V_{SL} + V_{SG}} \times 0.0234(m^3\,{}^{Kg}/_{KJ})P_{tot}$$

$$\frac{dm}{dP} = \frac{V_{SG}}{V_{SL} + V_{SG}} \times 0.0234(m^3\,{}^{Kg}/_{KJ})x_{H_2S}$$

also $U_x = 0.1$ from the tank certification sheet and $U_p = 0.033$ from the accuracy of the pressure gauge.

In the table below the column titled sample reading is the error percentage in which the scavenger's efficiency can be off by. This was done by doing one test multiple times, Figure 55 below, and taking and finding the standard deviation in which the values deviate from the mean.

Some other important uncertainties come from human error which is encountered when capturing the sample at the required times and the 1ppm resolution of the H_2S sensor being used.

Table 6: Table of Uncertainties

| Test #	Vsl	Vsg	σ (%) Liquid volume	σ (%) Sample Reading	σ (%) Pressure Reading	σ (%) Tank H2S Concentration	σ (%) H2S Mass Absorbed	σ (%) Watercut %	σ (%) Liquid Velocity
1	0.215	0.430	0.037	4.71	3.33	0.1	4.26	6.8	0.586
2	0.214	0.750	0.056	4.71	3.33	0.1	4.57	6.8	0.622
3	0.216	0.916	0.069	4.71	3.33	0.1	5.17	6.8	0.671
4	0.215	1.076	0.075	4.71	3.33	0.1	9.79	6.8	0.671
5	0.322	0.429	0.029	4.71	3.33	0.1	4.52	6.8	0.589
6	0.344	0.803	0.043	4.71	3.33	0.1	5.01	6.8	0.662
7	0.323	0.915	0.051	4.71	3.33	0.1	6.04	6.8	0.691
8	0.323	1.075	0.055	4.71	3.33	0.1	4.13	6.8	0.696
9	0.429	0.429	0.025	4.71	3.33	0.1	4.60	6.8	0.609
10	0.431	0.754	0.035	4.71	3.33	0.1	8.45	6.8	0.670
11	0.430	0.914	0.038	4.71	3.33	0.1	4.86	6.8	0.672
12	0.430	1.074	0.044	4.71	3.33	0.1	4.74	6.8	0.713
13	0.536	0.429	0.022	4.71	3.33	0.1	4.88	6.8	0.622
14	0.538	0.753	0.031	4.71	3.33	0.1	4.92	6.8	0.683
15	0.537	0.913	0.035	4.71	3.33	0.1	7.40	6.8	0.717
16	0.537	1.074	0.037	4.71	3.33	0.1	5.11	6.8	0.728
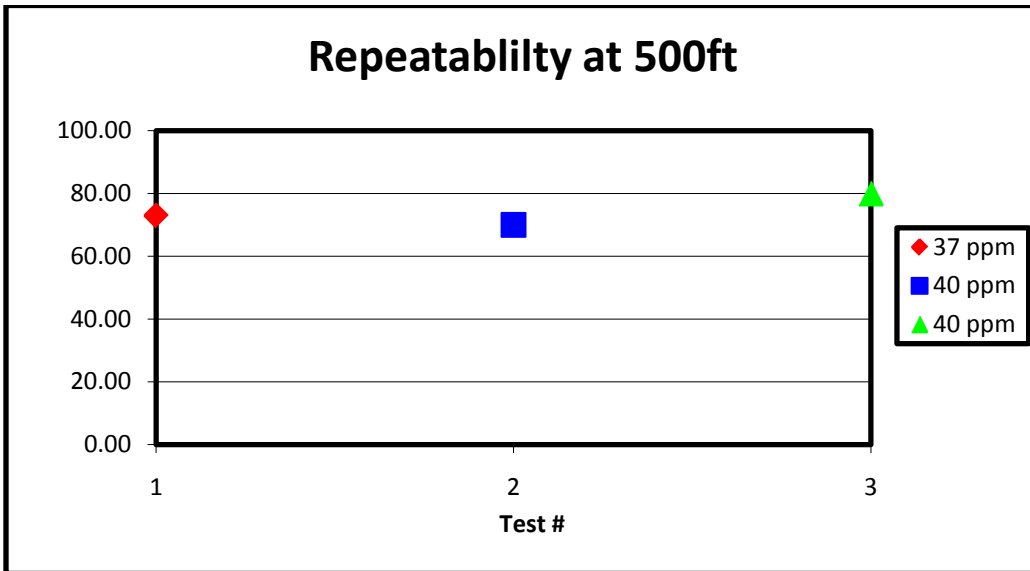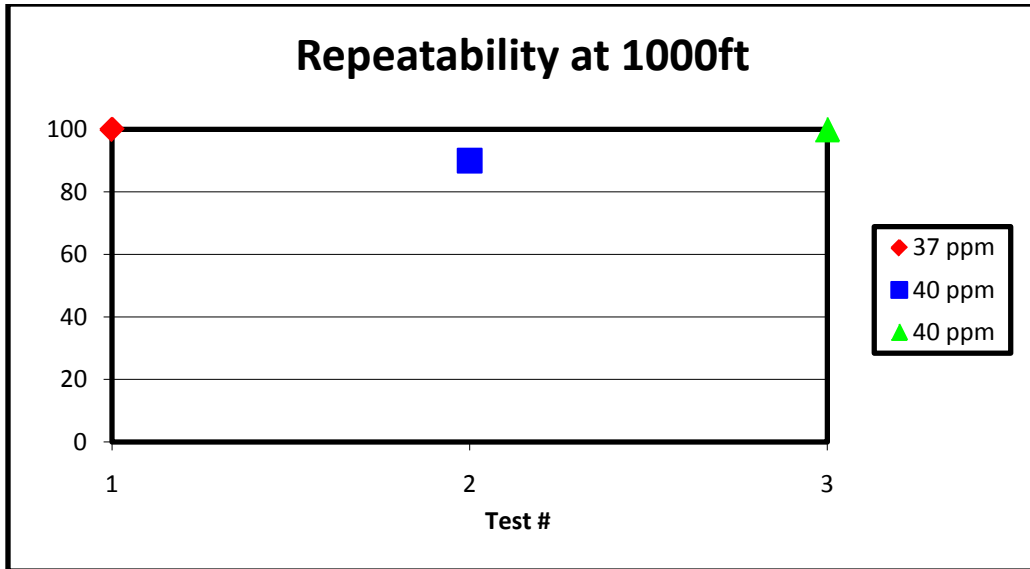
Figure 55: Repeatability of Efficiency; Vsl=0.215m/s, Vsg=0.43m/s. at 1000ft & 500ft
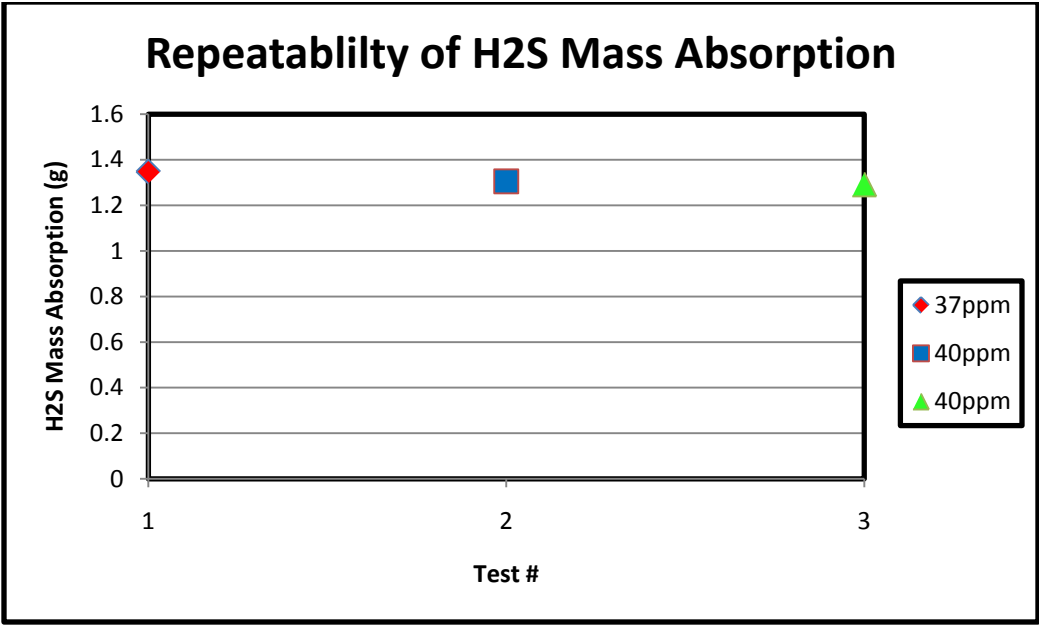
Figure 56: Repeatability for H2S Mass Absorption at Vsl = 0.215m/s and Vsg = 0.43m/s

LIST OF REFERENCES

[1] Hoffman, E.J., "Unsteady State Fluid Flow – Analysis and Applications to Petroleum Reservoir Behavior", Elservier Science B.V., The Netherlands, 1999, ISBN 0-444-50184-3

[2] Tver, D., Berry, R., "The Petroleum Dictionary", Litton Educational Publishing, USA, 1980, ISBN 442-24046-5

[3] Nguyen Phuong Tung., Pham Viet Hung., Hoang Dinh Tien., Cao My Loi., "Study of Corrosion Effect of H_2S Scavengers in Multiphase Systems" paper SPE 65399 presented at the 2001 SPE International Symposium on Oilfield Chemistry held in Houston, Texas, 13-16 February 2001.

[4] Chuanlian, Chen., Wenqin, Huang., "A Study of Sulfide Scavenger" SPE paper 14859 presented at the 1986 SPE International Meeting on Petroleum Engineering held in Beijing, China, March 17-20, 1986.

[5] Nagel, G., "Removing H_2S from Gas Streams" Report by U.S. Filter Gas Technology Products, USA.

[6] Zea, L., Kumar, R., Jepson P., "Role of Pressure and Reaction Time on Corrosion Control of H_2S Scavenger" paper SPE 114175-PP presented at the 2008 SPE Oilfield Corrosion Conference held in Aberdeen, UK, May 27, 2008.

[7]   Salma, T., "Effect of Carbon Dioxide on Hydrogen Sulfide Scavenging" paper SPE 59765 presented at the 2000 SPE/CERI Gas Technology Symposium held in Calgary, Alberta Canada, UK, April 3-5, 2000.

[8]   Sitz, C.D., Barbin, D.K., Hampton, B.J., "Scale Control in a Hydrogen Sulfide Treatment Program" paper SPE 80235 presented at the 2000 SPE International Symposium on Oilfield Chemistry held in Houston, Texas, February 5-7, 2003.

[9]   Salma, T., Baker, M.L., Herrmann, D.T., Yelverton, E.K., "Hydrogen Sulfide Removal from Sour Condensate Using Non-Regenerable Liquid Sulfide Scavengers: A Case Study" paper SPE 71078 presented at the 2001 SPE Rocky Mountain Petroleum Technology Conference held in Keystone, Colorado, May 21-23, 2001.

[10]   Wilson, D.R., "Hydrogen Sulphide Scavengers: Recent Experience in a Major North Sea Field" paper SPE 36943 presented at the 1996 SPE European Petroleum Conference held in Milan, Italy, October 22-24, 1996.

[11]   Dillon, E.T., "Composition and Method for Sweetening Hydrocarbons", United States Patent No. 4,987,512, (Dec 1990).

[12]   Castillo, M., Avila, Y.S., Rodrigues, R.E., Viloria, A., H_2S Liquid Scavengers, Their Corrosivity Properties and the Compatibility with others Down Stream Processes, NACE *Corrosion conference* 2000, Paper No. 00491.

[13]   Baldauff. J., Runge. T, Cadenhead, J. et al., Profiling and Quantifying Complex Multiphase Flow, *Oilfield Review*, Autumn 2004.

[14] Spedding, P.L., Cooper R.K., McBride, W.J., A Universal Flow Regime Map for Horizontal Two-Phase Flow in Pipes, *Dev. Chem Eng. Mineral Process*, vol 11, pp. 95-106, 2003.

[15] Annunziato, M., Abarbanel, H.D.I., "Nonlinear Dynamics for Classification of Multiphase Flow regimes", *Int. Conf. Soft Computing*, SOCO, Genoa, Italy 1999.

[16] Beretta A., Ferrari, P., Galbiati, L., Andreini, P.A., Horizontal Oil-Water Flow in Small Diameter Tubes. Flow Patterns, *Int. Comm. Heat Mass Transfer*, vol 24, No. 2, pp. 223-229, 1997.

[17] LIU Wenhong, GUO Liejin, Tiejun WU, ZHANG Ximin., An Experimental Study on the Flow Characteristics of Oil-Water Two-Phase Flow in Horizontal Straight Pipes, *Chinese J. Chem. Eng.*, vol 11, No. 5, pp. 491-496, 2003.

[18] Angeli, P., Hewitt, G.F., Flow structure in horizontal oil-water flow, *Int. J. Muti. Flow*, vol 26, pp. 1117-1140, 2000.

[19] Mishima, K., Hibiki, T., Some Characteristics of Air-Water Two-Phase Flow in Small Diameter Vertical Tubes, *Int. J. Muti. Flow*, vol 22, No. 4, pp. 703-712, 1996.

[20] Huo, X., Chen, L., Tian, Y.S., Karayiannis, T.G., Flow Boiling and Flow Regimes in Small Diameter Tubes, *Applied Thermal Engineering*, vol 24, pp. 1225-1239, 2004

[21] Oddie, G., Shi, H., Durlofsky, L.J., Aziz, K., Pfeffer, B., Holmes, J.A., Experimental Study of Two and Three Phase Flows in Large Diameter Inclined Pipes, *Int. J. Muti. Flow*, vol 29, pp. 527-558, 2003.

[22] Kang. C., Jepson. W.P., Wang, H., Flow Regime Transitions in Large Diameter Inclined Multiphase Pipelines, NACE *Corrosion conference* 2002, Paper No. 02243.

[23] Zhao, T.S., Bi, Q.C., Co-Current Air-Water Two-Phase Flow Patterns in Vertical Triangular Microchannels, *Int. J. Muti. Flow*, vol 27, pp. 765-782, 2001.

[24] Coleman, J. W., Garimella, Srinivas., Two-Phase Flow Regimes in Round, Square and Rectangular Tubes during Condensation of Refrigerant R134a, *Int. J. Refrigeration*, vol 2 pp. 117-128, 2003

[25] Chen, Xuejun., Guo, Liejin., Flow Patterns and Pressure Drop in Oil-Air-Water Three-Phase Flow Through Helically Coiled Tubes, *Int. J. Muti. Flow*, vol 25, pp. 1053-1072, 1999.

[26] Triplett, K.A., Ghiaasiaan, S.M., Abdel-Khalik, S.I., Sadowski, D.L., Gas-Liquid Two-Phase Flow in Microchannels Part I: Two-Phase Flow Patterns, *Int. J. Muti. Flow*, vol 25, pp. 377-394, 1999.

[27] Akbar, M.K., Plummer, D.A., Ghiaasiaan, S.M., On Gas-Liquid Two-Phase Flow Regimes in Microchannels, *Int. J. Muti. Flow*, vol 29, pp. 855-865, 2003

[28] Knudsen, B.L., Hjelsvold, M., Frost, T.K., Eiken, M.B.,Grini, P.G., "Toward Zero Environmental Impact of the Produced Water" paper SPE 83994 presented at the 2003 SPE Offshore Europe held in Aberdeen, U.K., September 2-5, 2003.

[29]   Sturman, P.J., Goeres, D.M., Winters, M.A., "Control of Hydrogen Sulfide in Oil and Gas Wells with Nitrite Injection" paper SPE 56772 presented at the 1999 SPE Annual Technical Conference and Exhibition held in Houston, Texas, October 3-6, 1999.

[30]   Kissel, C., Brady, J., Gottry, H., Meshishnek, M., Preus, M., "Factors Contributing to the Ability of Acrolein To Scavenge Corrosive Hydrogen Sulfide" paper SPE 11749, October 1985.

[31]   Hibiki, Takashi., Mishima, Kaichiro., Flow Regime Transition Criteria for Upward Two-Phase Flow in Vertical narrow Rectangular Channels, *Nuclear Engineering and Design*, vol 203, pp. 117-131, 2001

[32]   Henau, V.D., Raithby, G.D., A Study of Terrain-Induced Slugging in Two-Phase Flow Pipelines, *Int. J. Muti. Flow*, vol 21, No. 3, pp. 365-379, 1995

[33]   Corneliussen, S., Couput, Jean-Paul., et. al, "Handbook of Multiphase Metering", Norwegian Society for Oil and Gas Measurement, 2005, ISBN 82-91341-89-3

[34]   Paisley, D., Barret, N., Wilson, O., Pipeline Failure: The Roles Played by Corrosion, Flow and Metallurgy, NACE *Corrosion conference* 1999, Paper No. 18.

[35]   Mandhane, J.M., Gregory, G.A., Aziz, K., A Flow Pattern Map for Gas-Liquid Flow in Horizontal Pipes, *Int. J. Muti. Flow*, vol 1, pp. 537-553, 1974.

[36]   Dukler, A.E., 1978, Modeling Two Phase Flow and Heat Transfer, Keynote Paper KS-11, Proc. 6th Int. Heat Transfer Conf., Toronto, Canada.

97